33.5324.00/03/03 Confidential

REPORT

Seismic mapping and simulation of CO_2 migration in the upper Utsira sand wedge east of the Sleipner injection site

- A contribution to the Saline Aquifer CO_2 Storage (SACS) project

Martin Hamborg, Gary Kirby, Ane E. Lothe & Peter Zweigel

www.sintef.no

SINTEF Petroleum Research
June 2003

SINTEF

SINTEF

SINTEF Petroleumsforskning AS
SINTEF Petroleum Research

NO-7465 Trondheim

Telephone: (+47)73 59 11 00
Fax: (+47)73 59 11 02 (aut.)

Enterprise No.:
NO 936 882 331

REPORT

TITLE

Seismic mapping and simulation of CO_2 migration in the upper Utsira sand wedge east of the Sleipner injection site – A contribution to the Saline Aquifer CO_2 Storage (SACS) project

AUTHOR(S)

Martin Hamborg, Gary Kirby, Ane E. Lothe & Peter Zweigel

CLASSIFICATION	CLIENT(S)
Confidential	Statoil, SACS consortium, NFR-KLIMATEK
REPORT NO. 33.5324.00/03/03	

REG. NO.	DATE	PROJECT MANAGER	SIGN.
2003.032	11 June 2003	Peter Zweigel	*Peter Zweigel*
NO. OF PAGES	NO. OF APPENDICES	LINE MANAGER	SIGN.
42	1	Torleif Holt	*Torleif Holt*

SUMMARY

Previous work in the SACS project showed that injected CO_2 might migrate eastward and/or northward out of the mapped area of the reservoir unit. This study provides results of the seismic mapping of the reservoir top east and north of the area covered by 3D seismic data, and of migration simulations to predict CO_2 migration below the reservoir top.

Seismic mapping traced the top of a previously identified sand wedge at the top of the Utsira Sand east and northward of the injection site. It showed that this sand wedge is an integral part of the Utsira Sand and it is suggested here to clarify this in the nomenclature.

Simulation of the migration path of injected CO_2 showed that it will mainly migrate eastward from the point where it left the previously mapped area. Close to well 16/7-2, a domal trap is predicted to be filled which has a storage capacity of at least 77.2 Million m^3, corresponding to approximately 54 years of CO_2 injection at the present rate of 1 Million ton per year. Spill out of this trap is predicted to occur in eastward direction and to reach ultimately the eastern margin of the presently mapped area. Total trap volume on the whole simulated spill path is approximately 100 Million m^3.

The main practical consequences of these findings are that further detailed mapping of the top of the sand wedge towards east is not necessary, that well 16/7-2 will probably be reached by the injected CO_2, and that a baseline 3D seismic survey in the area of the domal trap may be useful for future monitoring.

KEYWORDS ENGLISH	KEYWORDS NORWEGIAN
North Sea	Nordsjøen
Sleipner field	Sleipnerfeltet
Carbon dioxide storage	Karbondioksidlagring
Seismic mapping	Seismisk kartlegging
Migration simulation	Migrasjonssimulering

Authors, Institutes, and Addresses

Martin Hamborg (Chapter 5)
Ane Lothe (Chapter 3)
Peter Zweigel (Chapters 1 – 6)

SINTEF Petroleum Research
S.P. Andersens vei 15 B
7465 Trondheim
Norway
Tel.: (+47) 7359 1100
Fax: (+47) 7359 1102
http://www.iku.sintef.no

Gary Kirby (Chapters 2 & 3)

British Geological Survey
Kingsley Dunham Centre,
Keyworth,
Nottingham NG12 5GG.
Tel: +44 (0)115 936 3100
Fax: +44 (0)115 936 3200
http://www.bgs.ac.uk/

Table of Contents

1. Executive summary

Previous work in the SACS project (Zweigel et al. 2000b) suggested the presence of two distinct reservoir units, the Utsira Sand proper and a slightly shallower, eastward thickening sand wedge, separated from the Utsira Sand by a 6-7 m thick shale layer. Simulation of buoyancy-driven CO_2 migration in the sand wedge (Zweigel et al. 2000a) predicted that the CO_2 would leave the previously mapped area at its eastern margin, approximately 7 to 10 km north-northeast of the injection site. Coarse mapping of the surrounding area based on scarce, widely spaced 2D seismic, indicated the possibility for eastward or north- to northwestward migration in the longer term, with the risk that potential sand stringers in downlapping cap rock sequences might be reached which might facilitate escape of CO_2 from the reservoir.

This study extends the mapped area towards east and north, based on additional, closely spaced seismic 2D data. Based on two new depth maps of the top sand wedge, migration simulations were carried out to predict long-term CO_2 migration pathways.

Seismic interpretation

The top of the sand wedge was mapped on 2D seismic lines east and north of the Sleipner CO_2 injection site. Detailed inspection, aided by wire-line log data, revealed that the shale layer between the sand wedge and the Utsira Sand, which has a constant thickness of approximately 6-7 m in the previously mapped area, thins and disappears towards east. There, the sand wedge is thus simply the uppermost part of the Utsira Sand and is one of several wedge-, lens- or sheetlike sand bodies in the Utsira Sand. Consequently, it is suggested that use of the term Sand Wedge is discontinued. The term “Upper leaf” of the Utsira Sand may be more appropriate.

The Utsira Sand as a whole was found to taper out in the extreme east. There is local downlap of shaley units in the east, but these are not thought to provide migration pathways for CO_2. There is a possibility however that sandy units may downlap and be in hydrological continuity locally in the north west, but the data is not of sufficient quality to be certain.

Time-depth conversion constrained by depth picks in nine exploration wells in the mapped area resulted in two slightly different versions of the top sand wedge depth map. Both versions show a general trend of a northward, in the northern part northwestward shallowing. This trend is overprinted by an irregular, roughly circular depression at the centre of the mapped area, which may cause eastward deflection of buoyancy-driven migration of the CO_2, which was predicted to enter the mapped area south of the depression.

Migration simulation

Two cases were simulated, one each for the two slightly different depth grids for the top of the sand wedge. Both cases yielded very similar results. In both cases, CO_2 is simulated to initially fill a domal trap directly around well 16/7-2 (Figure 1.1), close to

the position were CO_2 left the area of previous simulations (Zweigel et al. 2000a) and where it entered in the present ones. This trap has a pore volume of more than 77.2 Million m^3, corresponding to approximately 54 years of CO_2 injection at a rate of 1 Million ton per year. Maximum CO_2 column height in this trap prior to spill is simulated to be 26 m; however, this value might be different in reality because the present, simplified simulations neglect the possibility for a cone below the spill level.

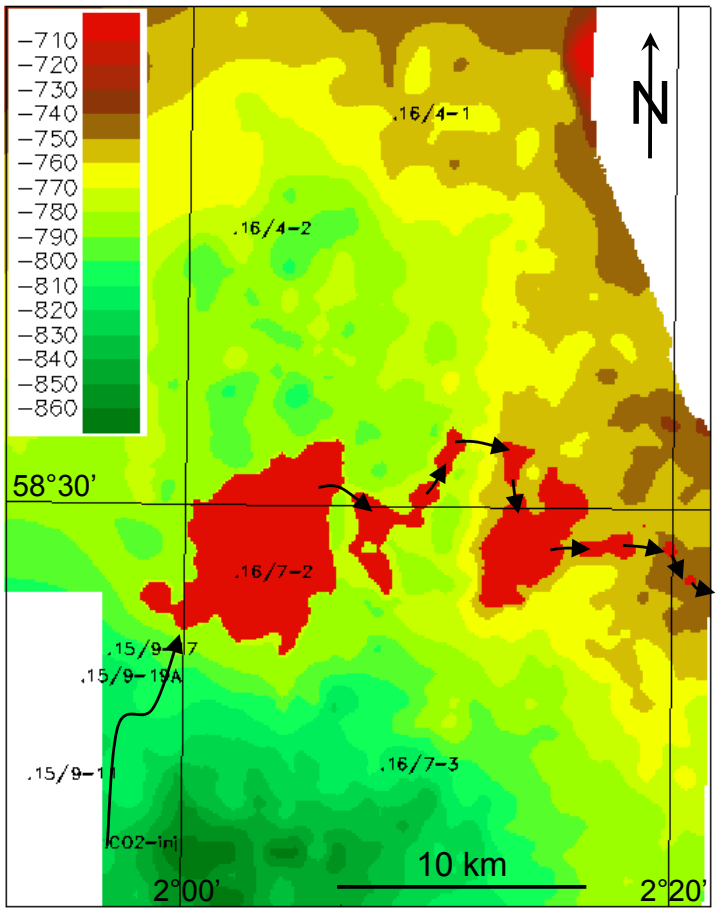

Figure 1.1 *Simulated CO_2 accumulations (red areas) in domal trap and migration path (arrows) towards eastern margin of mapped area. Migration path from CO_2 injection site into domal trap is schematically shown, too; details in Zweigel et al. (2000a). Case AQ, 105.8 Million m^3 CO_2 injected. Colour scale is depth to top sand wedge in m below sea level.*

Spill out of the domal trap is predicted to occur in eastward direction (Figure 1.1). Maximum trap volume on the whole spill path within the area of the simulated grids is 92 Million m^3 in one case and 105.8 Million m^3 in the other case. The calculated trap volumes make it unlikely that CO_2 injected at the present rate and planned time span will leave the mapped area. Further detailed mapping towards east therefore appears to be unnecessary.

Since exploration well 16/7-2 is predicted to be potentially reached by the CO_2 accumulating in the domal trap (Figure 1.1), it is advised that measures be taken to identify its leakage potential and – if necessary – to maintain its sealing capacity.

Seismic monitoring is the main, presently available method to monitor subsurface CO_2 migration and accumulation and to verify storage safety. A major prerequisite for seismic monitoring is a baseline survey, acquired prior to migration of CO_2 into the area of interest. If ongoing monitoring (especially the survey from 2003 and the one to be acquired in 2005) and related reservoir simulation should indicate that it will be likley that CO_2 will migrate out of the area of the existing 3D survey ST98M11 into the domal trap at well 16/7-2, a baseline survey covering the domal trap would be required.

2. Introduction

A detailed investigation of the reservoir geology of the storage units for CO_2 sequestration in the Sleipner field (Zweigel et al, 2000b), utilising 3D seismic (survey ST98M11), scarce, widely spaced 2D seismic, and well data, led to the model presented in Figure 2.1. This suggested the presence of two reservoir units; the main body of the Utsira Sand and a "sand wedge" lying approximately 6-7 m above this unit within the lowermost Nordland Shales. The sand wedge was so named because of its apparent eastward thickening nature.

Results of the SACS time-lapse seismic surveys acquired in 1999 and 2001 (Arts et al., 2003) suggest that CO_2 had migrated into this "sand wedge" through the shale that separates this from the main body of the Utsira Sand. Simulation of the migration of CO_2 within the sand wedge (Zweigel et al, 2000a) indicates that the direction of migration would be to the north or northeast, in contrast to the northwestward direction at the top of the main body of the Utsira Sand. This northeastward migration path would take the CO_2 out of the 3D data area at a distance of 7 to 10 km from the injection site; hence the full path and ultimate fate of the CO_2 could not be determined. It was thought possible that migration within the sand wedge could take the CO_2 eastward to the toes of westward prograding wedges of sediment and thus provide pathways to the sea floor in the eastern part of the basin. It was strongly recommended therefore that further mapping be done to determine the full migration path, using all available data. These data (exclusively 2D) were located and requested by SINTEF to be made available for this study and were supplied by Statoil.

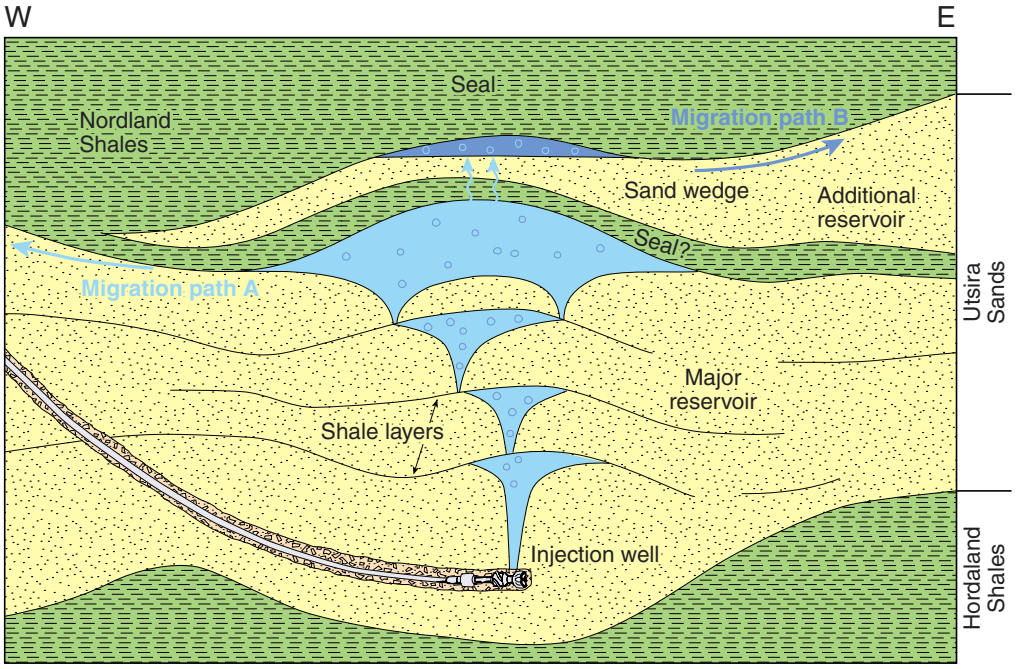

Figure 2.1 Schematic reservoir model for the Sleipner CO_2 injection case based on previous geological work and reservoir simulations (adapted from Zweigel et al. 2000b). The right hand column shows the revised interpretation based on the present report.

This report details work based on this extra data, integrated with a re-interpretation of some of the previously available 2D data. Work carried out consisted of three main parts, results of which will be presented separately below:

- Mapping of the top of the "sand wedge" and of its lithostratigraphic equivalent on 2D seismic data.
- Gridding and time-depth conversion of the mapped horizon into a 3D depth grid.
- Simulation of CO_2 migration below the top of the mapped horizon.

Gridding, time-depth conversion, and migration simulation were restricted to the data from the 2D surveys and did not combine the previous top sand wedge data from the 3D survey with the new 2D interpretation. This was done because local misfits between the different data types were difficult to eliminate and they would have caused artefacts in the depth grid that would have affected migration simulation results. Instead, the results of the previous migration simulation (Zweigel et al, 2000a), especially the end point of the previously modelled migration path, were used as input for the new simulations.

3. Seismic interpretation

3.1 Data

A total of six 2D surveys were identified that would be of use in the mapping of the top Sand wedge. A list of these data, together with comments on their quality is presented in Table 3.1 and Table 3.2. The distribution of these data with respect to the 3D and 4D data areas is shown in Figure 3.1. Of these data sets, the NH8008, NH8105, E82 and NH8601 datasets have the closest line spacing and provide the best areal coverage. The CNST82 and VGST89 data provide additional, but more widely spaced control.

The NH8008 survey was taken as the "standard" survey and it was found that several of the surveys required a time shift to be applied to the lines to obtain a character match. The amount of this shift is indicated in Table 3.1. There was also a misfit between the standard survey NH8008 and the 3D survey ST98M11.

Table 3.1 2D seismic surveys used in the interpretation

Surveys	Quality	Shift	Polarity
E82	Excellent	-12 ms	Normal
NH8008	Good	used as standard (but lines19, 20, 21, 22 shifted by -12 ms)	Normal
NH8105	Variable, good to poor, especially in north	0	Reversed
NH8601	Poor	0	Normal
CNST82	Poor to good	-12 ms	Normal
VGST89	Good	-12 ms	Normal

Table 3.2 Seismic 2D lines used for interpretation

Survey name	Lines used
E-82	559, 561, 563, 565, 567, 569, 571, 573A, 573, 742A, 742, 744, 746, 748
NH8008	1, 2, 3, 4, 5, 6, 7, 8, 9, 10, 11, 12, 13, 14, 15, 16, 17, 18, 19, 20, 21, 22, 23, 24, 25
NH8105	124, 125-A, 125, 202-A, 202, 303-A, 303, 304, 305-A, 305, 306, 307, 307-A, 308, 309, 310-A
NH8611	201B, 201A, 202D, 202A, 203, 204, 205A, 206A, 206, 207, 208A, 401B, 402, 403
CNST82	05B, 06, 07, 07X, 18, 19
VGST89	104, 105, 105A, 107, 108, 109, 111, 201B, 201C, 202B, 202C, 203, 204

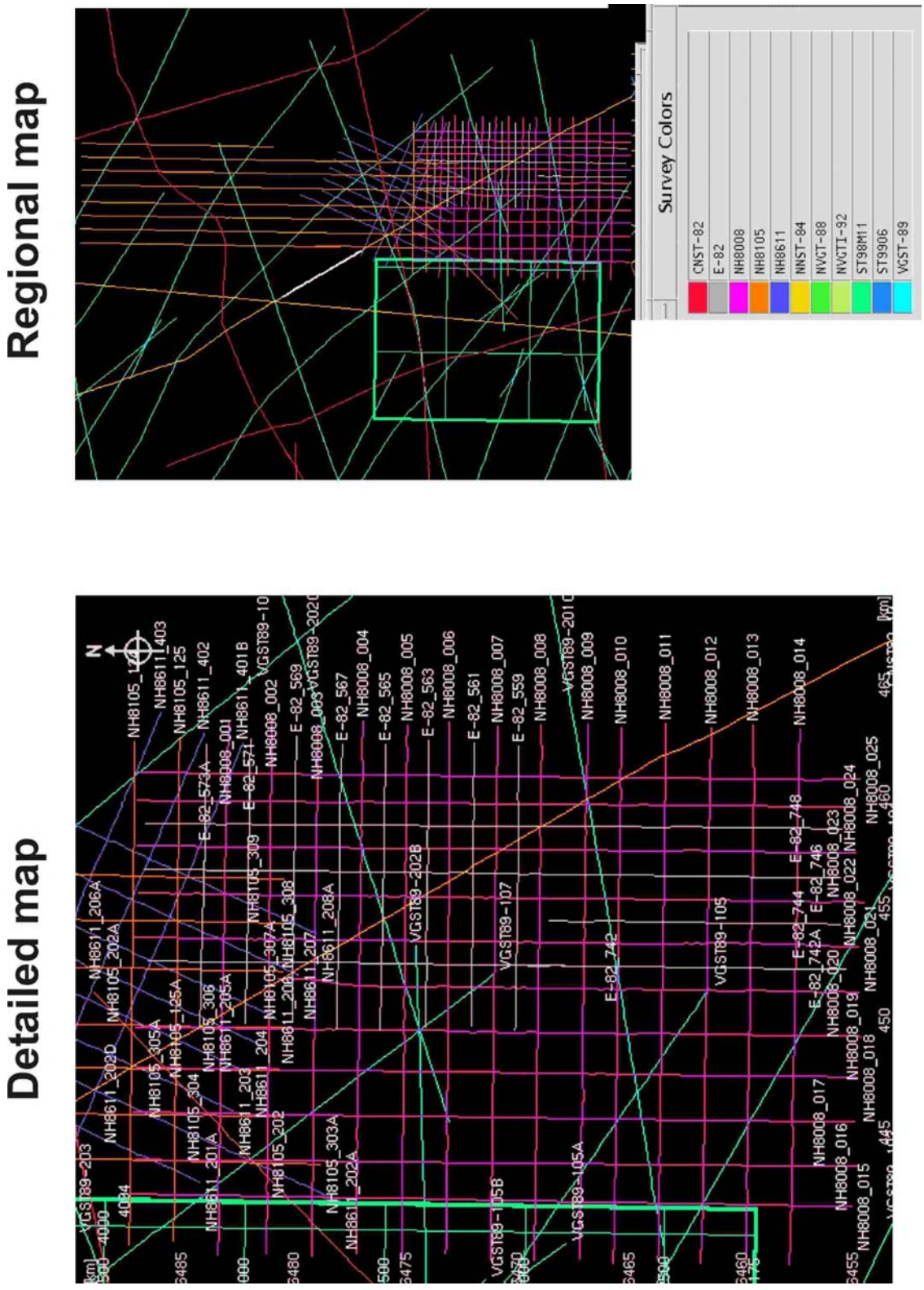

Figure 3.1 *Base map of the interpreted 2D lines with respect to the previously interpreted 3D seismic survey ST98M11.*

3.2 Interpretation

The top of the Utsira Sand and of the sand wedge are characterised by a downward decrease in sonic velocity and density. Consequently the pick for both these horizons is on a blue peak on the seismic data (Figure 3.2).

The relationship between the top Utsira Sand pick and the top Sand Wedge pick towards the western margin of the Sand Wedge is clear on the 3D data, with the Sand Wedge pick becoming progressively less distinct westwards until it cannot be traced further. This is interpreted (Zweigel et al. 2000b) as indicating progressive westwards thinning of the Sand Wedge to a thickness below seismic resolution and eventually to zero, as indicated by well logs. There is no evidence of downlap of the Sand Wedge onto the top Utsira pick. The relationship of this western margin on 2D data is generally less clear, although can be interpreted in exactly the same way. A comparison of data quality between the 3D and 2D data can be seen in Figure 3.2.

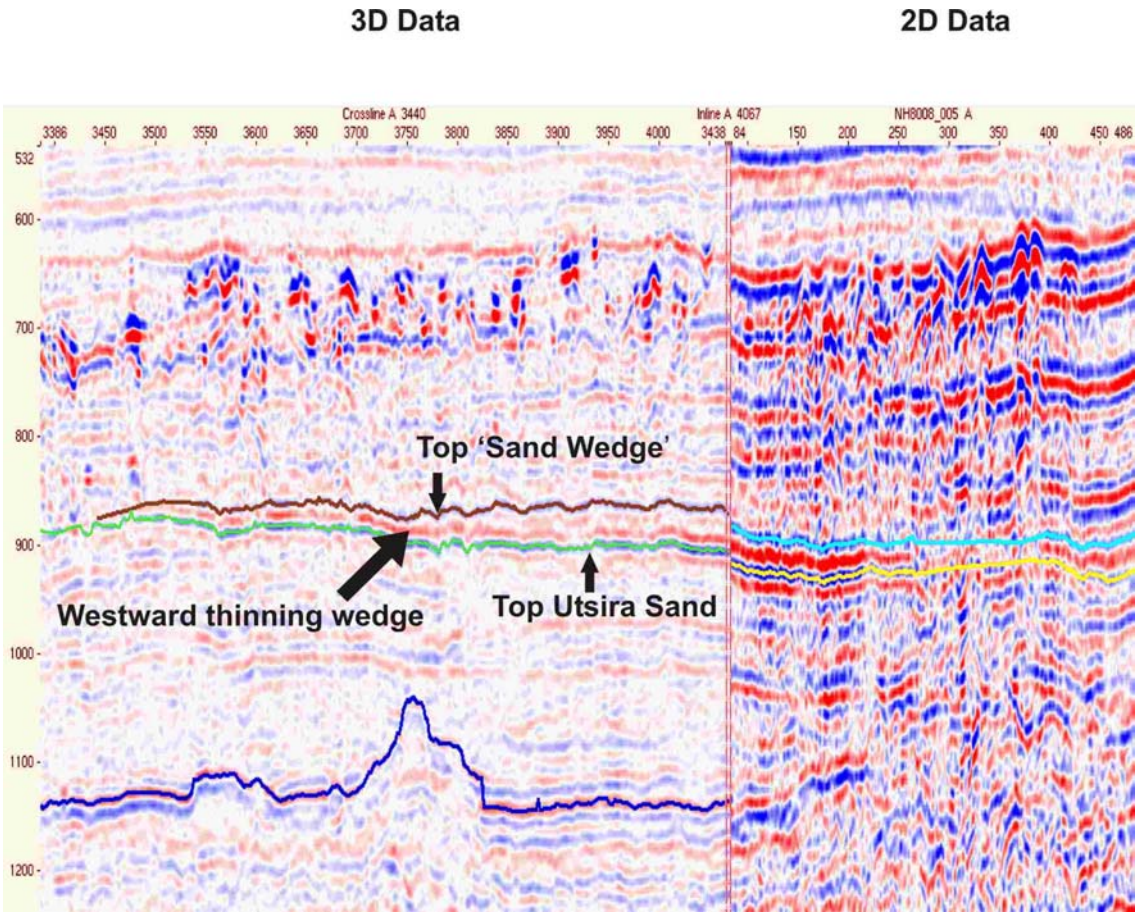

Figure 3.2 *Comparison of 3D and 2D data quality: note time shift between surveys. Also note eastward thickening of wedge on 3D data changes to eastwards thinning on 2D data. 3D data: crossline 3440 of survey ST98M11. 2D data: line NH8008-005. Note use of "Top Utsira Sand" according to previous definition.*

The top Utsira Sand pick remains strong for a certain distance eastwards under the Sand Wedge pick, before becoming progressively less distinct until ultimately it cannot be traced with confidence. The intervening amplitude trough between the peaks of the Sand Wedge and top Utsira Sand increases both in amplitude and in time thickness towards and just beyond the eastern edge of the 3D data before decreasing in amplitude eastwards as the top Utsira Sand pick becomes weaker. This change in character is attributed to "tuning" effects of events at the top of the Sand Wedge and the top and base of the underlying shale and is thought to indicate eastward thickening of the sand wedge in the west and eastward thinning of the intervening shale in the east. Where the top Sand Wedge becomes "unpickable" in the west it is thought that the sand wedge is below seismic resolution. Similarly, where the top Utsira becomes "unpickable" in the east it is thought that the intervening shale is below seismic resolution. This is confirmed by the westward thinning of the sand wedge and eastward thinning of the shale observed in well logs. The point at which the top Utsira pick and/or the top sand wedge pick cannot be traced further depends also on data quality – on poorer data it is difficult to be consistent. However, using the NH8008 data, "holes" in the area of extent can be mapped, and are thought to represent areas with particularly thin shale unit between the top Sand Wedge and top Utsira.

Where the intervening shale is very thin, the top of the Sand Wedge is effectively the top of the major sand body i.e. the top of the Utsira Sand; but at a slightly higher stratigraphic level. This is the general situation in the east and north of the area.

In the extreme east, it is the top Sand Wedge pick at the top of the Utsira Sand that laps out against a rising mid Miocene onlap surface. Beyond this point, there is no Utsira Sand present (Figure 3.3). Locally in the east, there is slight downlap observed onto the top Sand Wedge (Figure 3.4). Wells 16/ 7-1 and 16/8-1 however indicate that this downlap is entirely within a shale succession, with no indication of sand bodies that could provide a pathway for migrating CO_2.

In the northwest, the marginal relationships of the Sand Wedge are unclear, being seen only on two seismic lines, both of poor quality (Figure 3.5). It is possible however that the Sand Wedge merges into the local downlapping succession of the "western prograding unit", which is thought to be sand prone. If this is the case then this could potentially provide a migration pathway for CO_2 if it were to migrate this far.

Locally in the north of the study area, the top Sand Wedge pick becomes indistinct for a short distance (Figure 3.6). It is thought that this may be due to a downcutting channel within the Nordland shale. The uniform low amplitude nature of the data in the channel fill suggests that this fill may also be shale and that there is no possible migration pathway for CO_2 out of the Sand Wedge.

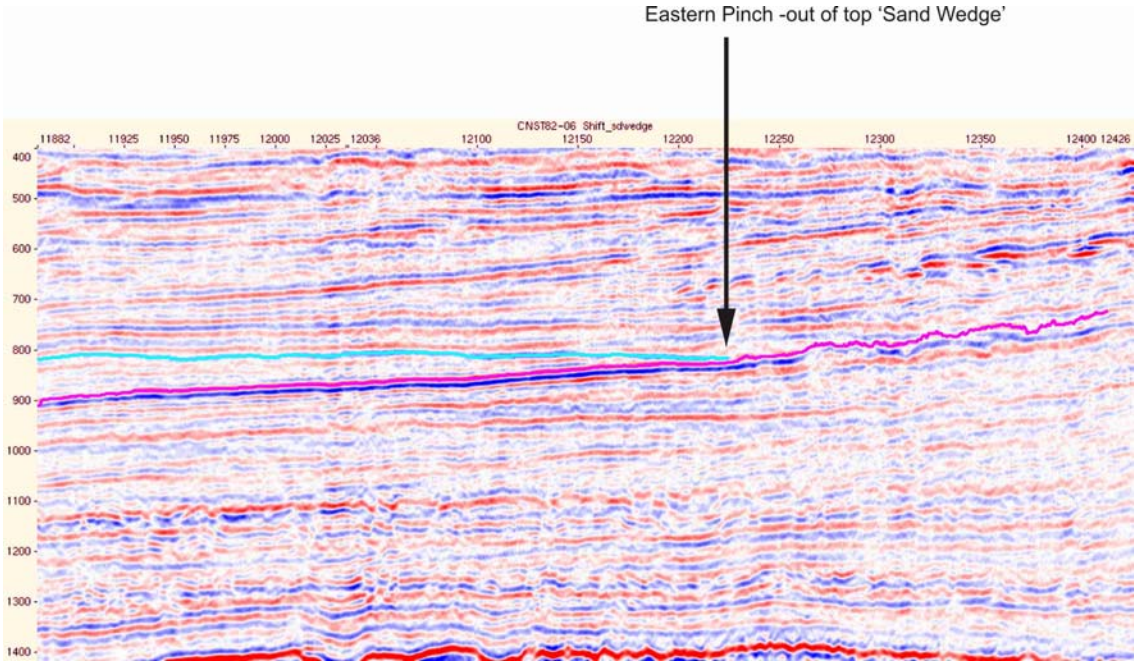

Figure 3.3 *Eastern pinch-out of top Sand Wedge reflection at top of Utsira Sand, against rising mid Miocene onlap surface. Also note local minor downlap onto the top Sand Wedge near its eastern limits. Line CNST92-06.*

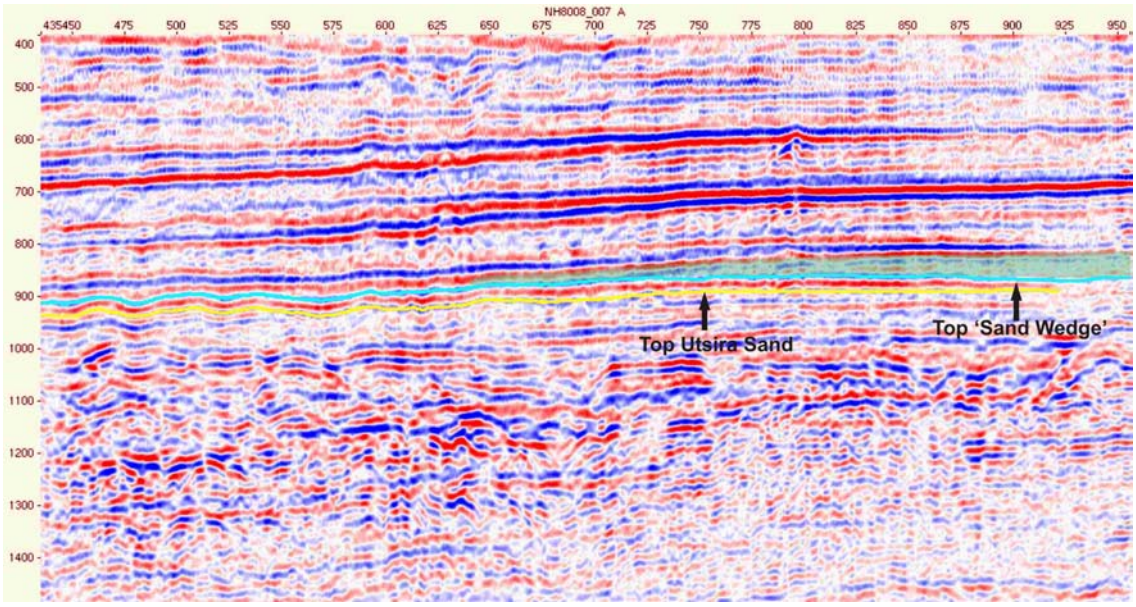

Figure 3.4 *Local low angle downlap onto top Sand Wedge reflection, highlighted by green shaded wedge-like unit. Line NH8008-007. Note use of "Top Utsira Sand" according to previous definition.*

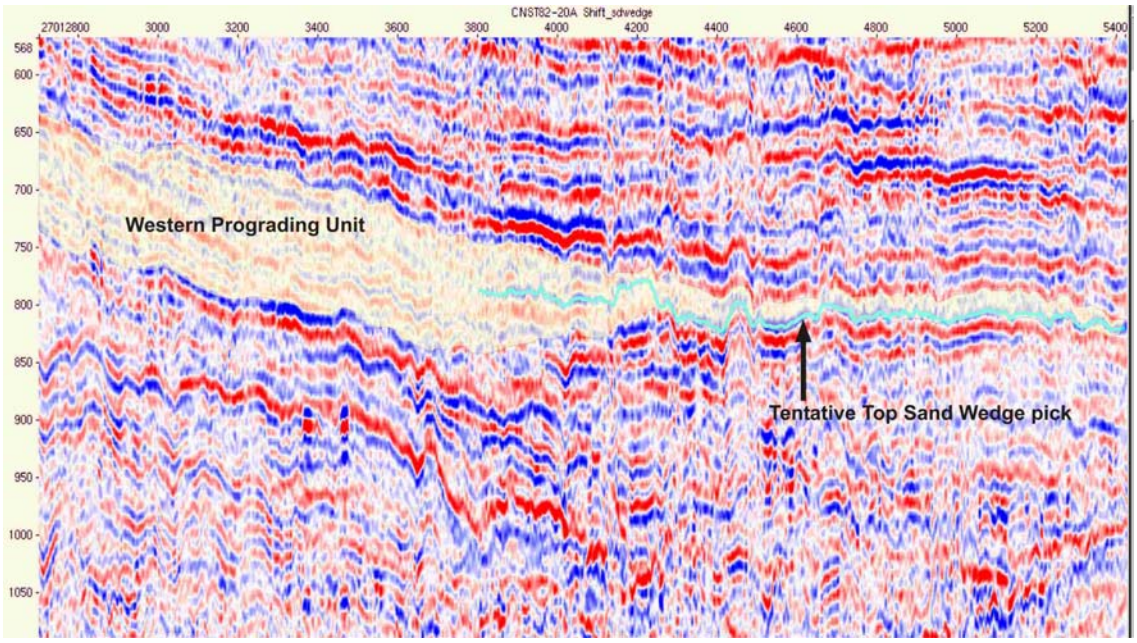

Figure 3.5 *Tentative relationships between top Sand Wedge reflection and "Western Prograding Unit", thought to be sand prone. Reflection appears to run into this prograding unit; however, pick is uncertain due to poor quality data. Line CNST82-20A.*

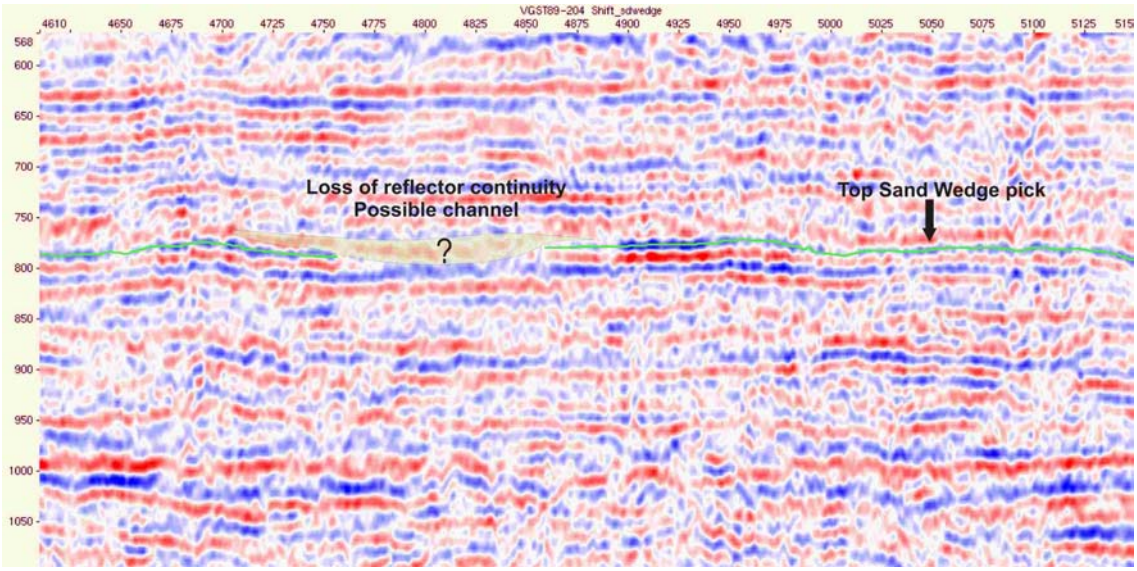

Figure 3.6 *Local loss of strength of top Sand Wedge reflection, possibly due to downcutting channel. Line VGST89-204.*

These observed relationships permit the generalised model presented in Figure 3.7 to be constructed. It can be seen that the Sand Wedge is in effect an upper "leaf" of the Utsira Sand, which is only present in the east of the basin and which is structurally conformable with the remainder of the Utsira Sand, and in general with the lower part of the overlying Nordland Shale (the "Shale drape"). The intervening shale unit, approximately 6-7 m thick in the west is thought to thin eastwards to be indistinguishable from any other shale break within the Utsira Sand. At this point, the top of the Sand Wedge effectively becomes the top of the Utsira Sand body, which is therefore younger in the east than in the west. For this reason, it is suggested that use of the term Sand Wedge is discontinued, as this implies a significant genetic difference between this and the Utsira Sand, which is not supported by this study. The term "Upper leaf" of the Utsira Sand may be more appropriate.

There is local downlap of shaley units in the east, but these are not thought to provide migration pathways for CO_2. There is a possibility however that sandy units may downlap and be in hydrological continuity locally in the northwest, but the data is not of sufficient quality to be certain.

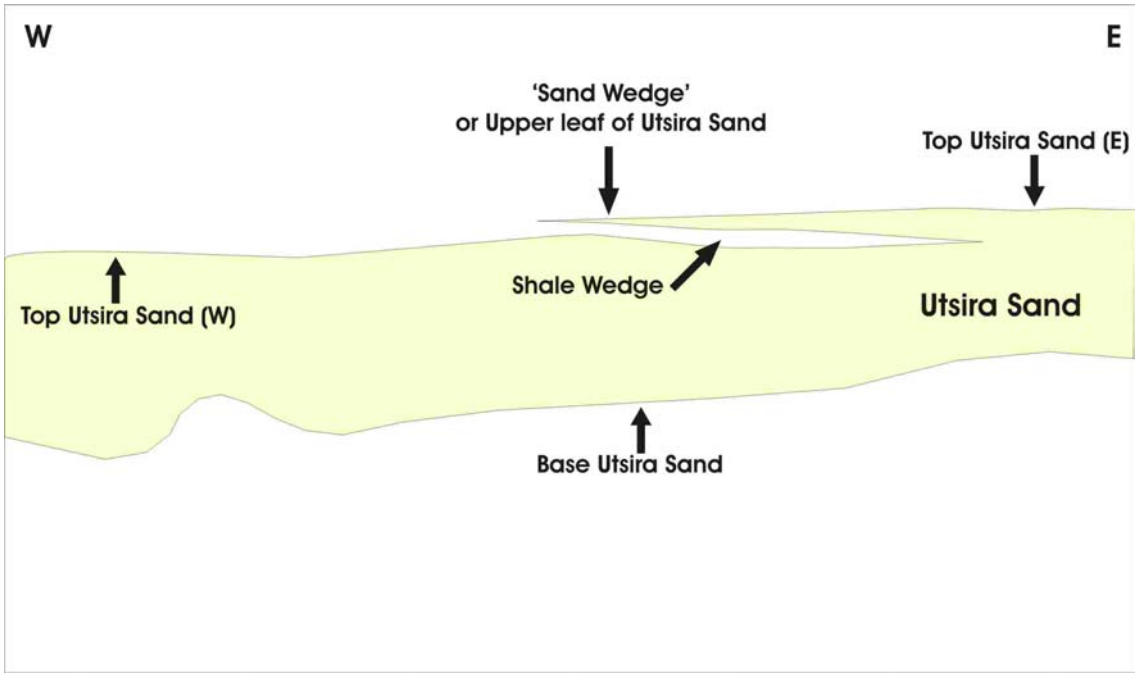

Figure 3.7 *Revised model for the Utsira Sand. The "Sand Wedge" is in effect the topmost "leaf" of the Utsira Sand, such that the top of the Utsira Sand in the east is younger than that in the west.*

4. Time-depth conversion

Time-depth conversion consisted essentially of three steps:

- Gridding of the top sand wedge horizon as interpreted from 2D seismic lines (previous Chapter) into a regular surface.
- Collection and quality check of depth data for the top of the sand wedge from wireline log data.
- Depth conversion of the gridded top sand wedge horizon constrained by the well data.

Each of these steps is documented in chapters below.

4.1 Time horizon gridding

Horizon gridding was carried out employing Geoframe-Charisma's "Grid Utility" module. First, a regularly spaced grid, covering the area of interest, was defined with a grid cell spacing of 100 m in both UTM-east and UTM-north directions (Table 4.1). Then the interpreted horizon segments on the selected seismic lines (Table 3.2) were gridded, using the "strong" gridding modus of the software, applying a manually defined outer boundary around the area covered by data, and not applying any smoothing.

The resulting two-way travel time (TWTT) grid had large extreme positive and negative values in some areas weakly constrained by input data. These values were removed, as were data outside the defined outer boundary. The resulting, "cleaned" TWTT grid has still surprisingly low values in the NNW, around line CNST82-07 (CDPs 3300 – 3600). The gridding is, however, in accordance with the interpretation of the segment in 2D, and the deeper position of the interpreted horizon there might be due to a change of the reflector depth in the seismic data (processing or acquisition artefact).

The "cleaned" TWTT grid was then filtered to remove imprints of individual lines and of slight inconsistencies at some line intersections. Filtering was done by a median filter, covering a 5·5 grid cell area, applying it once only (no iteration). The resulting TWTT grid is shown in Figure 4.1.

Table 4.1 Properties of the grid library used for time-depth conversion of the 2D top sand wedge horizon.

Property	Value
Origin, UTM-east	4150000
Origin, UTM-north	64545000
Cell length east-west	100m
Cell length north-south	100m
Nr. of cells east-west	486
Nr. of cells north-south	766

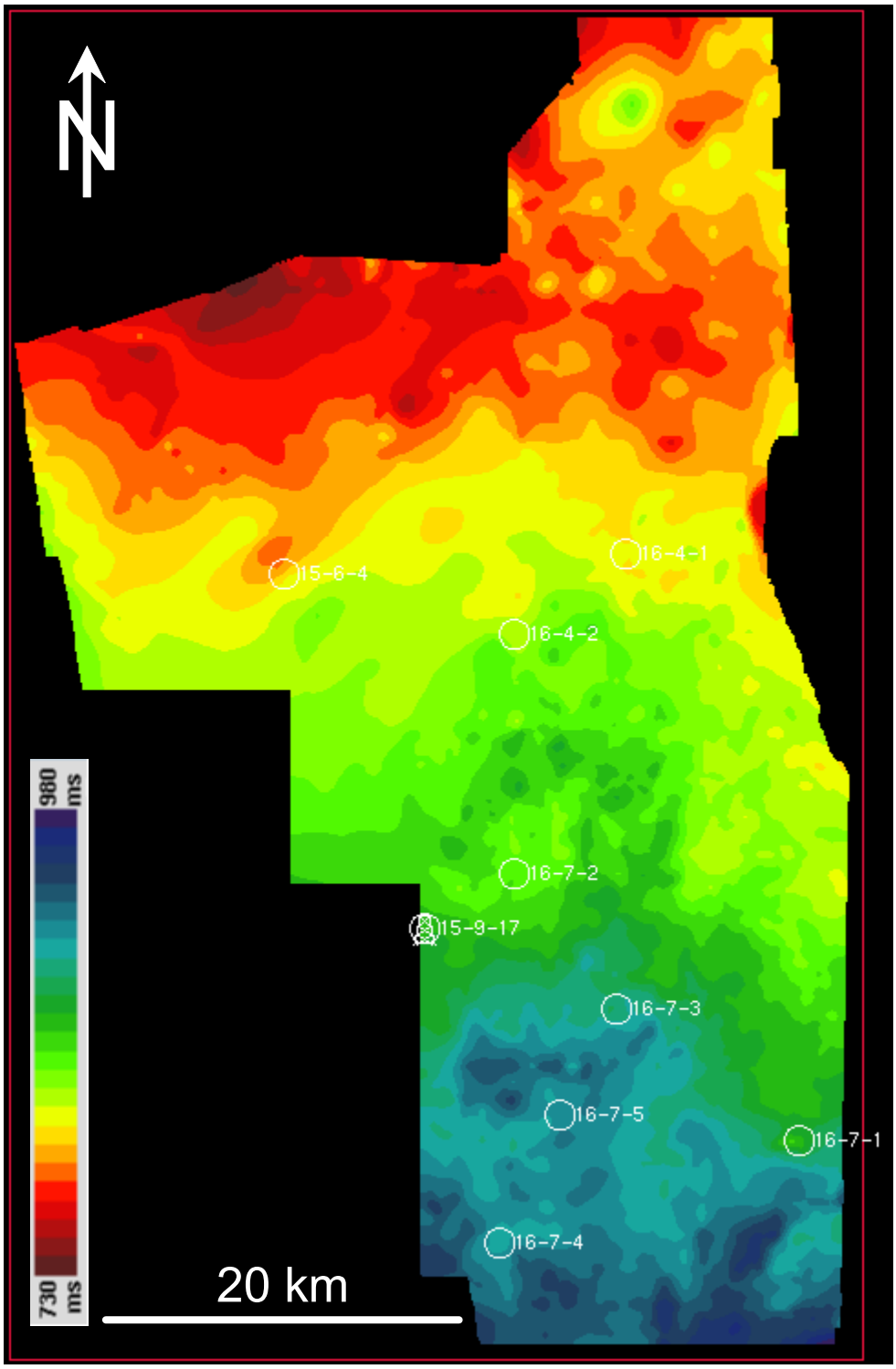

Figure 4.1 Filtered two-way travel time grid of the top sand wedge horizon.

4.2 Depth data from wells

The top of the sand wedge was interpreted on wireline logs from nine wells situated in the area of the interpolated grid. The Utsira Sand and the sand wedge at its top are easily recognizable on wire-line logs by a strong downward decrease of gamma-ray (GR) log values, marking the transition from the overlying Nordland shale to the Utsira Sand. In the case of the sand wedge being present, a package of a few meters thickness (up to approx. 30m) with low GR values is underlain by a 6-7 m thick package of higher GR, which in turn is underlain by a package of approximately 200 – 300 m thickness with mainly low GR values and a few, thin spikes of high GR (Zweigel et al. 2000, their Figure 5.7). Positions of the wells and the depth of the top of the sand wedge are given in Table 4.2.

Table 4.2 Wells used for time-depth conversion of the top of the sand wedge, and depth of the top sand wedge in these wells.

Well	UTM-east	UTM-north	Depth (TVDss, m)	Comment
15/6-4	430618	6499093	720.4	
15/9-17	438602.8	6478955	809.94	
16/4-1	449960	6500262	760	top Utsira
16/4-2	443619.4	6495668	778	top Utsira
16/7-1	459826.9	6466867	783.5	
16/7-2	443667.1	6482040	769	
16/7-3	449482.5	6474397	810	
16/7-4	442832.3	6461118	823	
16/7-5	446286.7	6468385	841.24	

4.3 Time-depth conversion procedure

Time-depth conversion employed the Geoframe InDepth program module. Input data were the filtered two-way travel time (TWTT) grid of the top sand wedge horizon (Chapter 4.1) and the depth of the top sand wedge in the nine wells listed in Table 4.2. Time-depth conversion was carried out using an average overburden velocity.

In a first step, average overburden velocities were calculated for each well, and from them, a regional average of average overburden velocities was determined (Table 4.3). The TWTT grid was then depth converted into a depth grid (AJ) using this regional average velocity of 1835 m/s.

In a second step, the misfit between the calculated depth grid and the horizon depth at the well positions was determined, and correction factors for each well were calculated to achieve fit (Table 4.4).

The correction factor data points were then gridded into a correction factor grid, using the "Radial Basis (Duchon spline)" modus of the software, applying no smoothing. The resulting correction factor grid (AP, Figure 4.2a) has large extremes in weakly constrained area, reaching values far above and below the range of the correction factors at the well positions.

To assess the effect of the extremes, and to remove them, a second gridding of the correction factor data point was carried out with the same procedure as the previous one, but with additional, manually inserted control points of value 1 (i.e. no correction of the depth grid at these points) added (Figure 4.2c, Table 4.5). The resulting, constrained correction factor grid (AR) is shown in Figure 4.2b.

Table 4.3 Average overburden velocities (and input data) at the nine wells used for time-depth conversion.

Well	Depth (TVDss, m)	TWTT at well (ms)	Vp (m/s)
15/6-4	720.4	801	1798.8
15/9-17	809.94	868	1866.2
16/4-1	760	814	1867.3
16/4-2	778	826	1883.8
16/7-1	783.5	865	1811.6
16/7-2	769	848	1813.7
16/7-3	810	891	1818.2
16/7-4	823	904	1820.8
16/7-5	841.24	915	1838.8
		average:	1835

The original depth grid (AJ) was then corrected to yield fit at well positions, by multiplication with the unconstrained and the constrained correction factor grids. This resulted in two corrected depth grids, AQ from the unconstrained correction factor (Figure 4.3), and AS from the constrained one (Figure 4.4). Note that well control is weak in the northern part of the study area, and that the depth grids there have a larger uncertainty than in the central and southern parts.

Table 4.4 Correction factors to be applied during time-depth conversion to achieve depth fit at well positions.

Well	Correction parameter
15/4-1	1.01730
15/4-2	1.02632
15/6-4	0.97922
15/9-17	1.01685
16/7-1	0.98680
16/7-2	0.98880
16/7-3	0.99089
16/7-4	0.99199
16/7-5	1.00259

Table 4.5 Position of manually inserted control points with correction factor 1.0

UTM East	UTM North
416506	6511263
419770	6492930
432073	6516159
444255	6516409
448652	6529597
457690	6529595
458445	6515780
461458	6456139

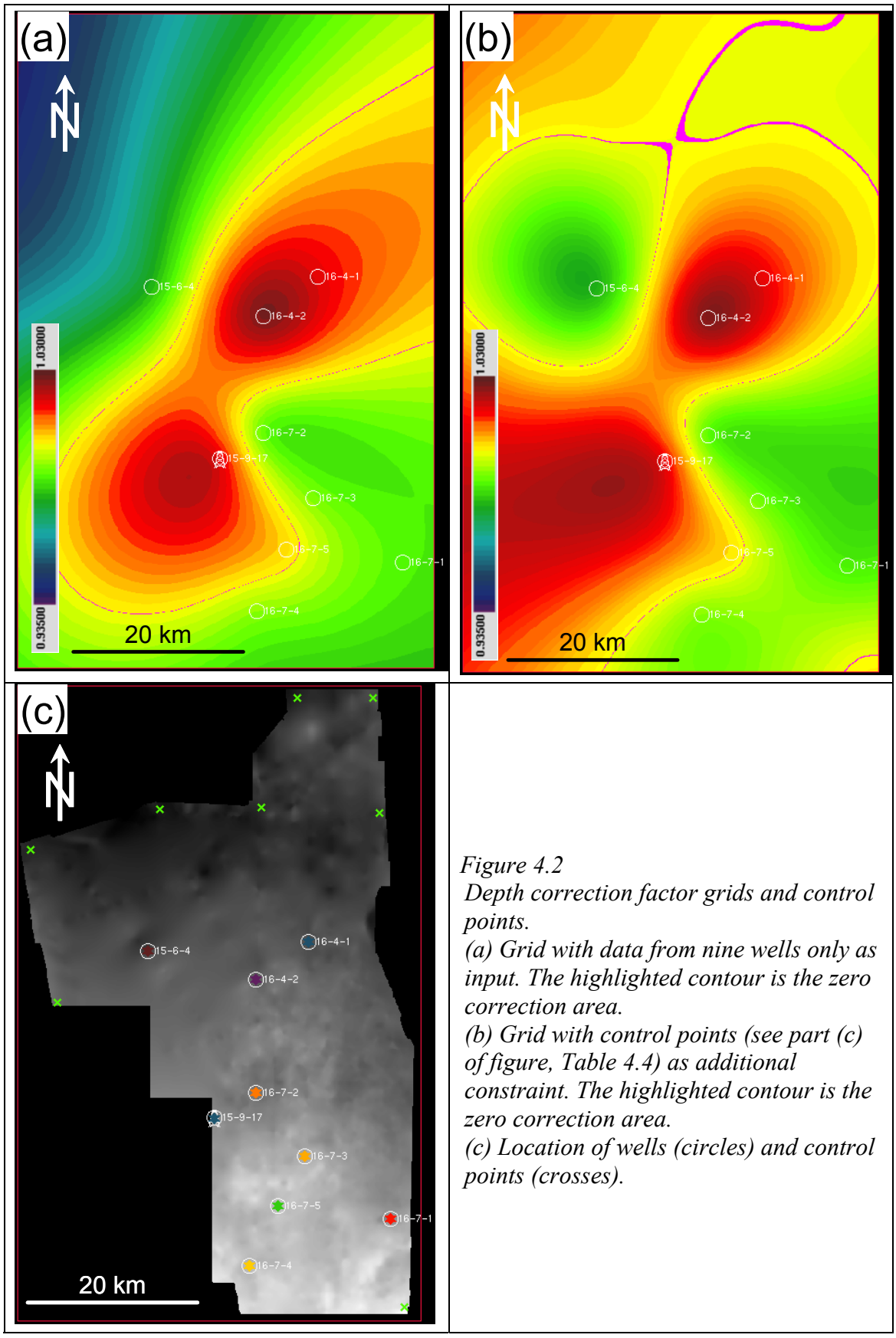

Figure 4.2
Depth correction factor grids and control points.
(a) Grid with data from nine wells only as input. The highlighted contour is the zero correction area.
(b) Grid with control points (see part (c) of figure, Table 4.4) as additional constraint. The highlighted contour is the zero correction area.
(c) Location of wells (circles) and control points (crosses).

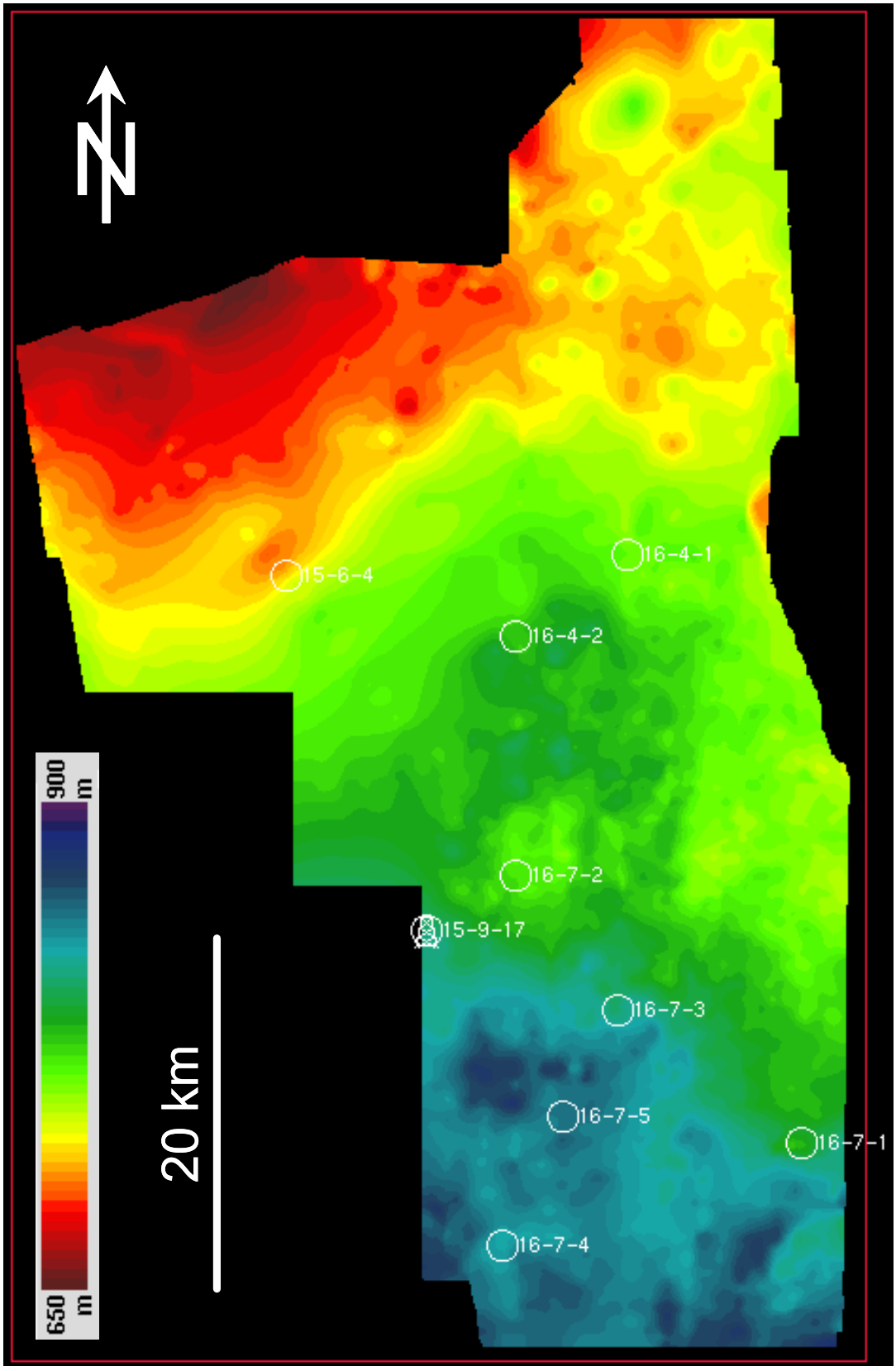

Figure 4.3 *Depth to top sand wedge (grid AQ) employing unconstrained correction factor grid (Figure 4.2a) to reach fit at well positions.*

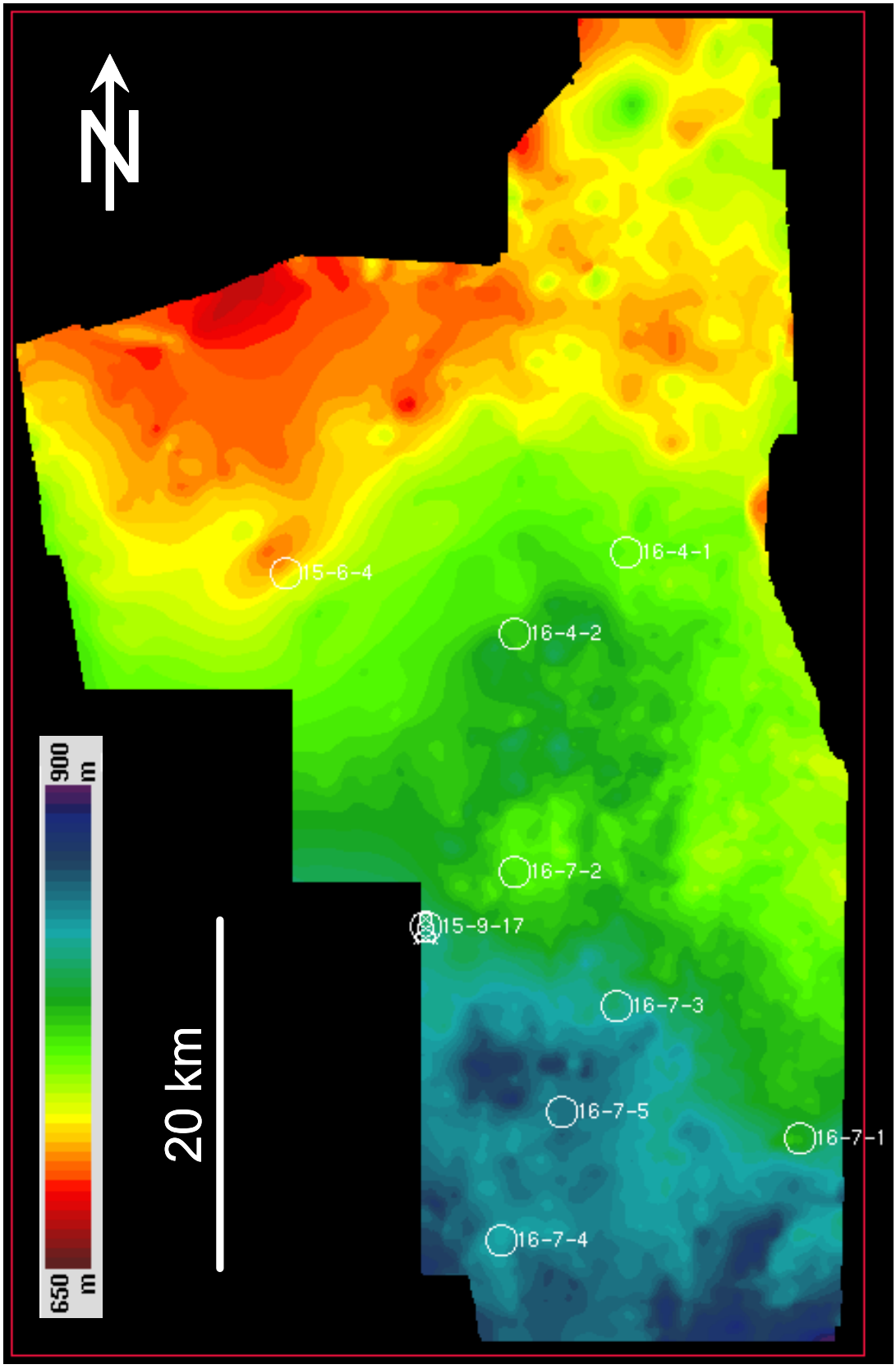

Figure 4.4 *Depth to top sand wedge (grid AS) employing correction factor grid constrained by manually inserted control points (Figure 4.2b) to reach fit at well positions.*

4.4 Depth grids

The two depth grids (Figure 4.3 and Figure 4.4) have many features in common, differences being largely restricted to the north-westernmost part (Figure 4.5). The main trend of the depth grids is a northward shallowing, in the northern part a northwestward shallowing. This trend is overprinted by an irregular, roughly circular depression at, and south of, well 16/4-2, and a domal high around well 16/7-2. The domal high is partly due to the existence of lows around it, which are at least in the east a consequence of pronounced subsidence due to compaction of a mud edifice at the base of the Utsira Sand (compare with such structures presented and explained in Zweigel et al. 2000a). The depression around well 16/4-2 is at least partly introduced by time-depth conversion, as shown by comparison of the two-way time map (Figure 4.1) with the depth maps (Figure 4.3 and Figure 4.4), and by inspection of the correction factor grids which illustrate velocity variation across the area.(Figure 4.2a&b). The depression can however not simply be discarded as an artefact, because the time-depth conversion honours the depth in well 16/4-2 correctly, i.e. at least at the well, the top sand wedge is at the same depth as in the depth maps. The real shape and areal size of the depression may though differ from that in the grids in Figure 4.3 and Figure 4.4. This may have consequences for the validity of the migration simulations of the next chapter (see discussion there).

As mentioned before (Chapter 4.1), a local dome in the northwesternmost part of the grid may be due to seismic data artefacts.

Since migration simulation (next chapter) will incorporate results from the previous migration simulation (Zweigel et al. 2000a) which used a depth grid of the top sand wedge horizon based on 3D seismic data (“3D grid”, Figure 4.6), and since the new grids (“2D grids”) and the 3D grid overlap, it is worth to inspect their mutual fit.

Similarly to the 2D grids, the 3D grid has a tendency of northward shallowing. The 3D grid (Figure 4.6) shows an area of reduced depths northeast of well 15/9-17, which corresponds to the domal high around well 16/7-2 in the 2D grids. A flank into a depression east of the injection site in the 3D grid corresponds to a depression in the 2D grids directly NW of well 16/7-5.

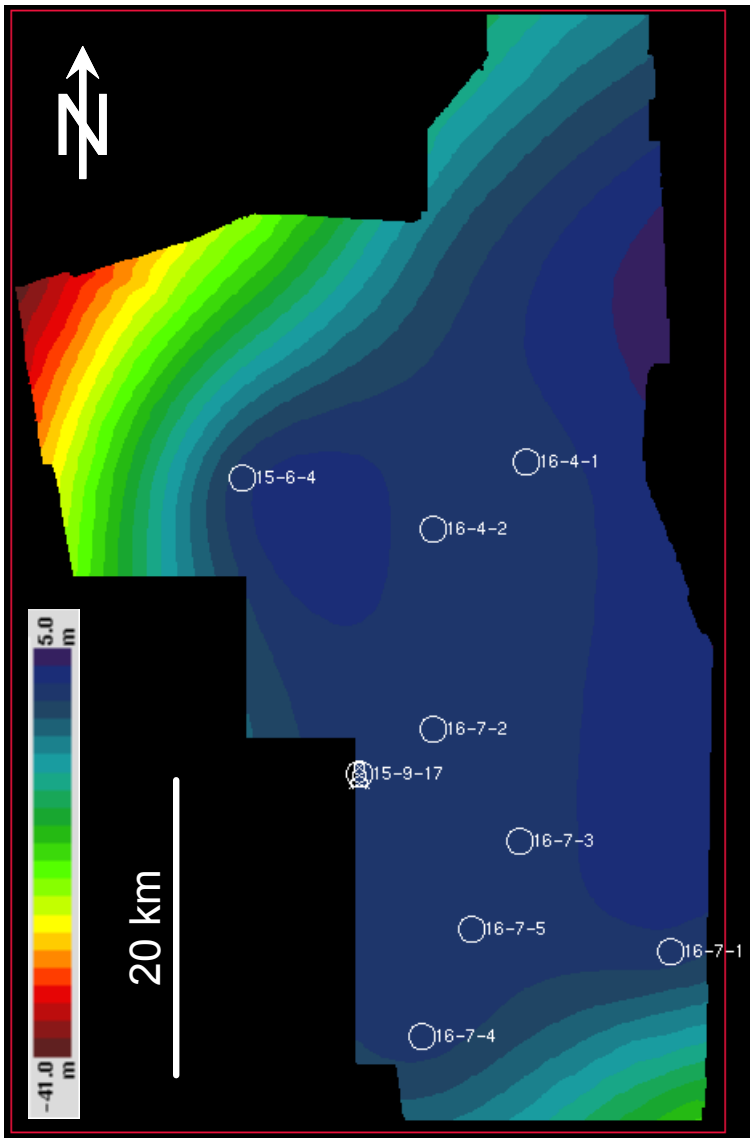

Figure 4.5 *Depth difference between depth grid AQ (wells as input only; Figure 4.3) and depth grid AS (with additional control points, Figure 4.4).*

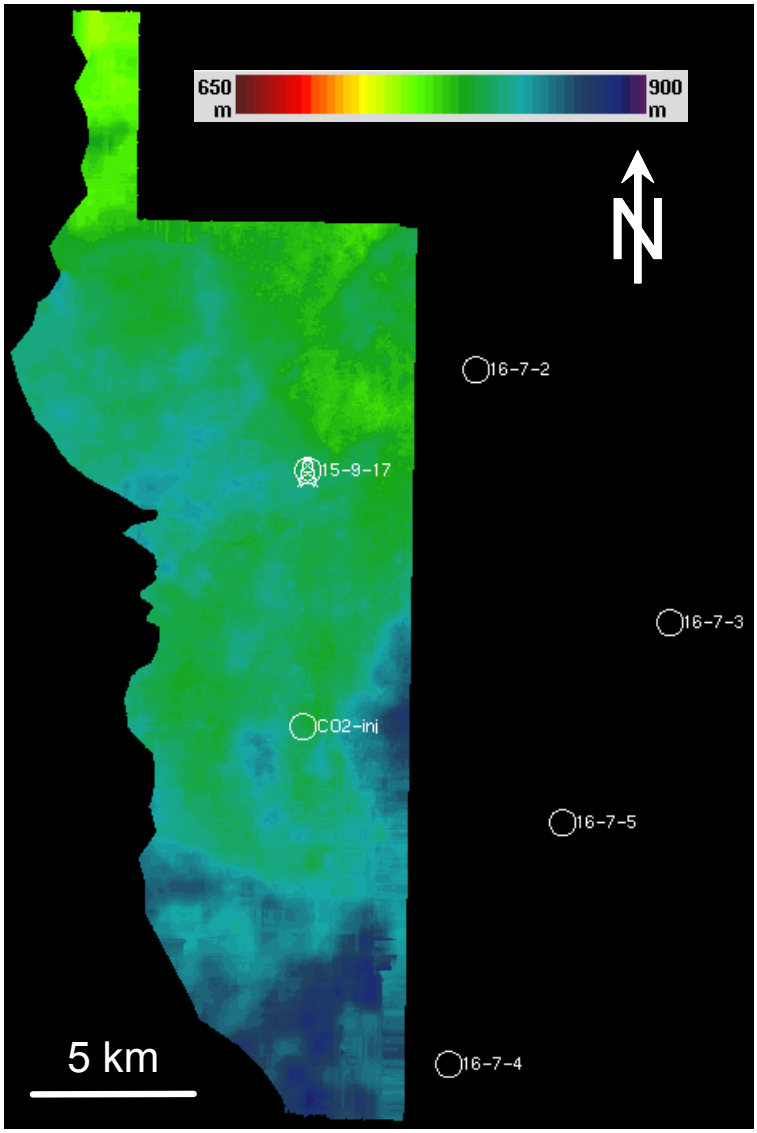

Figure 4.6 *Depth to top sand wedge as interpreted on 3D seismic survey ST98M11. This depth horizon ("3D grid") was used for the previous simulation of CO_2 migration in the sand wedge (Zweigel et al. 2000a). Note the different depth scale as compared to Figure 4.3 and Figure 4.4.*

5. Migration simulation

5.1 Methodology

The migration simulations were carried out using SINTEF Petroleum Research's in-house developed secondary hydrocarbon migration simulator SEMI (Sylta 1991). SEMI is a program for performing buoyancy-driven secondary migration of oil and gas along horizon maps in 3 dimensions. The main migration work is performed using a ray-tracing procedure to simulate what is considered to be a very fast drainage migration from one or more sources into their nearest traps. Thereafter, spillage of the migrating phase is modelled from deeper traps into shallower traps, depending on whether each trap can hold the phase that migrates into it or not. Buoyancy is considered the main driving force causing fluid movement in these simulations and the topography of barriers and carriers is accordingly the primary parameter influencing migration. Migration is treated to occur in layers below barriers (seals) instead through whole rock volumes.

We used only basic functions of SEMI, e.g. loss of CO_2 by solution, capillary and/or hydraulic leakage was not considered, nor did we include effects of changing temperature and pressure during migration; we modelled migration in single layer cases; and we did not include variations of porosity or permeability within the reservoir/carrier beds. Consequently, reservoir top (or base seal) topography is the main controlling factor on the migration pattern in the studied cases and SEMI is thus able to test the influence of topography on the predicted subsurface CO_2 distribution.

5.2 Simulation parameters

The input parameters for the simulations are listed in Table 5.1.

Two main simulation runs were carried out, one for each of the two top sand wedge depth grids (Grid AS and Grid AQ). No base grid for the sand wedge was used. The sand wedge has a maximum thickness of at least 26 m, which it reaches in well 16/7-2, i.e. within the area of the simulated accumulation (see below). The maximum CO_2 column height simulated was 26 m, too.

The entry point for the CO_2 in the simulations was the point at which CO_2 left the grid area of the previous simulations (Zweigel et al. 2000a, case W-2) which covered the CO_2 migration from the injection site in well 15/9-A23 in the area of the seismic 3D survey ST98M11.

Porosity and Net-Gross ratio are the same as in the previous simulations (Zweigel et al. 2000a) and are in accordance with evaluations by Zweigel et al. (2000b) and Zweigel et al. (2003 in prep). The density of CO_2 in the subsurface is the same as in previous simulations and is based on calculations documented in Lindeberg et al. (2000).

Simulation steps are multiples of the annual injection rate at Sleipner (1 Million tons CO_2 corresponding to 1.43 Million m^3 at reservoir condition). The first steps are with small differences, to cover the planned injection interval (approximately 20 years) in

detail. Note that 7.4 Million m^3 are already stored in traps (Zweigel et al. 2000a) before reaching the start point of the present injection. Later steps are large and have the main purpose to determine the general topographic trend for the case that CO_2 injection might continue for more than 20 years.

Table 5.1 Input parameters for CO2-migration simulation.

Parameter	**Value**
Top carrier grid	Depth grid AD (Case AS) Depth grid AQ (Case AQ)
Base carrier grid	unlimited
Entry point for CO_2	UTM 440992 E UTM 6478716 N
Porosity	30%
Net-Gross ratio	0.85
Density of CO_2 in reservoir	700 kg/m^3
Injection steps (in cumulative Million m^3/yr at subsurface conditions)	2.86, 5.72, 8.58, 11.44, 14.3, 17.16, 20.02, 22.88, 34.3, 48.6, 62.9, 77.2, 91.5 Case AS: 92.0 Case AQ: 105.8

5.3 Simulation results

The simulation results are documented in map view in Appendix A. The two cases (AS and AQ) yield almost identical migration results. The main differences are in the first step and in the very last steps, and in the total stored volume along the migration path.

In both cases, CO_2 is simulated to initially fill a domal trap directly northeast of, and including, well 16/7-2 (Figure 5.1) , close to the position were CO_2 left the area of previous simulations (Zweigel et al. 2000a) and where it entered in the present ones. The centre of this trap is at a distance of approximately 14 km from the injection site. It has a diameter of approximately 7.5 km; its top is at 753 m TVDss. The trap has a pore volume of more than 77.2 Million m^3. Maximum CO_2 column height in the trap prior to spill is simulated to be 26 m.

Spill out of the domal trap is predicted to occur in eastward direction (Figure 5.2). Maximum trap volume on the whole spill path within the area of the simulated grids is 92 Million m^3 in case AS and 105.8 Million m^3 in case AQ.

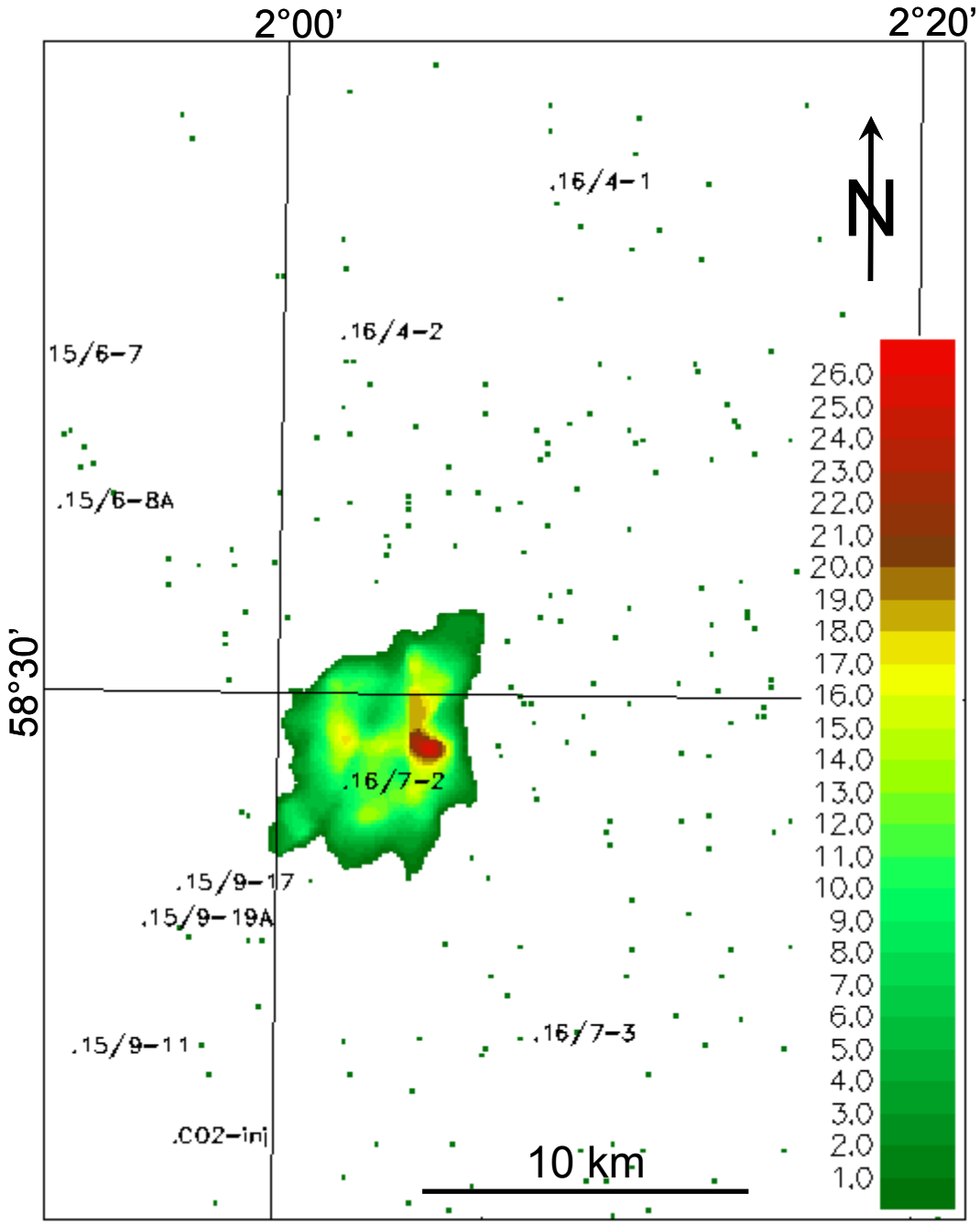

Figure 5.1 *Simulated CO_2 accumulation in map view and column height in domal trap northeast of well 16/7-2, shortly prior to spill out of trap. Case AQ, 77.2 Million m^3 CO_2 injected. Colour scale is CO_2 column height in m.*

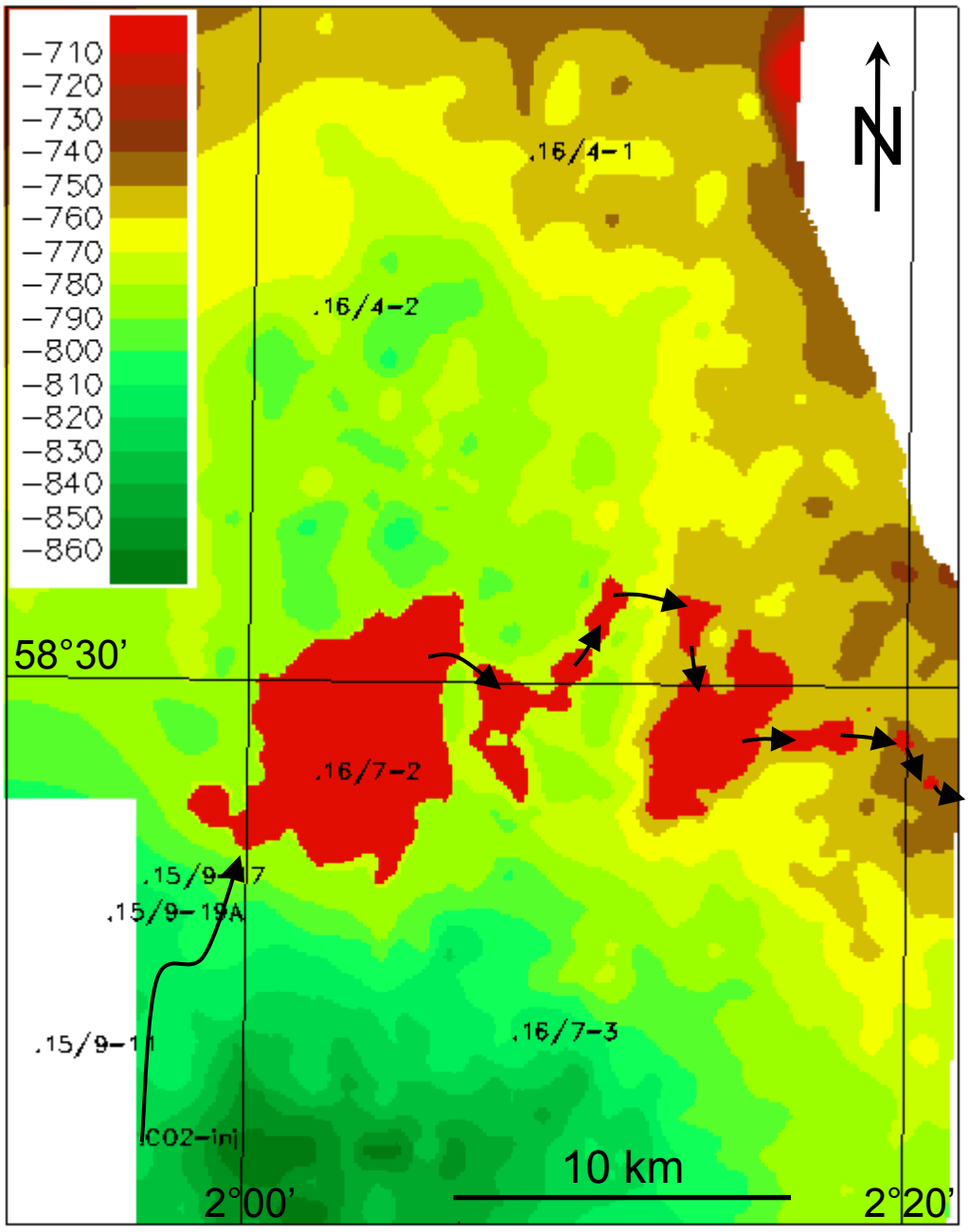

Figure 5.2 *Simulated CO_2 accumulations (red areas) in domal trap and migration path (arrows) towards eastern margin of mapped area. Migration path from CO_2 injection site into domal trap is schematically shown, too; details in Zweigel et al. (2000a). Case AQ, 105.8 Million m^3 CO_2 injected. Colour scale is depth to top sand wedge in m below sea level.*

6. Discussion and conclusions

Uncertainty

The identified domal trap has its top at 753 m TVDss (in both grids AS and AQ). Its calculated spill level is at 779 m TVDss, yielding a maximum column height (assuming a horizontal base of the CO_2 accumulation) of 26 m. However, both seismic interpretation and time-depth conversion introduce uncertainties affecting the depth grids used for simulation.

Figure 6.1 shows the difference of the depth of the trap horizon from the level of the trap top. For both cases simulated (case AQ and AS), alternative spill paths, causing migration towards northwest, are 8 m deeper than the simulated spill path towards east. Spill through these paths may results in migration of CO_2 far towards northwest, following the topography of the reservoir top (Figure 4.3, Figure 4.4).

The alternative, northwestward spill paths are approximately 17 m deeper than the expected base of the CO_2 accumulation if all CO_2 after 20 years of injection would accumulate in the domal trap. In reality, the CO_2 accumulation may not have a horizontal base and spill points deeper than the simulated ones may be reached. We consider, however, the depth difference of 17 m between the simulated accumulation base and the northwestward spill path to be sufficient to prevent migration in that direction.

For comparison, a simple time-depth conversion was carried out, applying the average seismic velocity of 1835 m/s (Table 4.3) to the filtered two-way travel time (TWTT) grid (Figure 4.1). The result is shown in Figure 6.1c. In this case, the trap top is at 764m TVDss, spill level is at 781 m TVDss and the maximum column height (assuming a horizontal accumulation base) is 16 m. Note that spill in this case would occur towards northwest.

The difference between the simulated cases and the depth grid from simple time-depth conversion is caused by the non-uniform, laterally variable seismic velocity used in the time-depth conversion procedure presented in Chapter 4. In this advanced procedure, a zone of low seismic velocity (grid correction factors <1) is present at well 16/7-2 and east of it, and a zone of high velocity (grid correction factor >1) stretches in a northeasterly direction between wells 15/9-17 and 16/4-2, northwest of the domal trap (Figure 4.2). This introduces “lifting” of the depth grids AQ and AS at and east of well 16/7-2 and a depression northwest of this area. Even though the precise shape and extent of these velocity features is not known, their presence is necessary because depth data in the wells require velocities differing from well to well to achieve fit of the mapped seismic horizon at the well positions. In conclusion, we consider the advanced cases (cases AQ and AS) to be more likely than the depth grid from simple time-depth conversion.

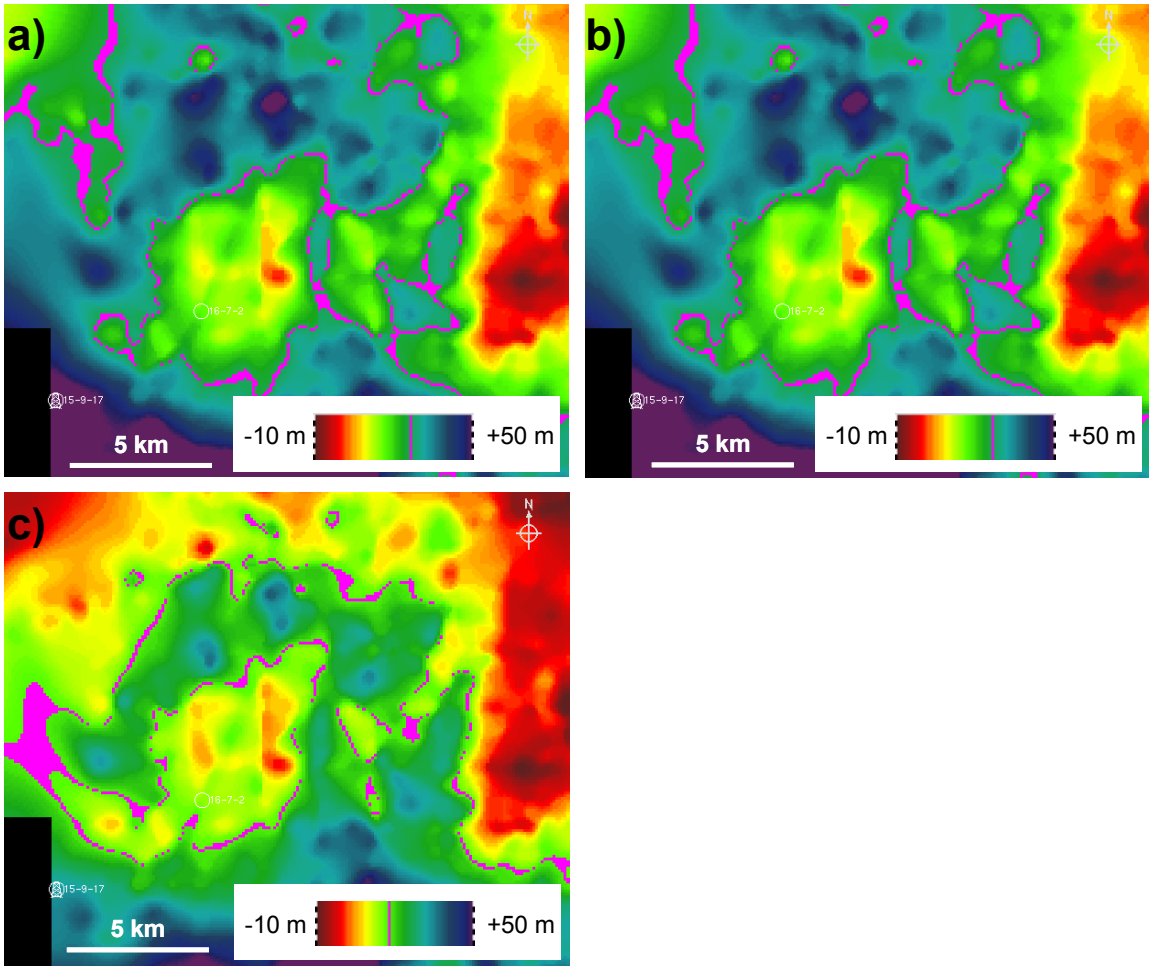

Figure 6.1 *Depth difference of depth grids to top of domal trap in m. a) Grid AQ. b) Grid AS. c) Depth grid from simple time-depth conversion, applying uniform velocity of 1835 m/s to filtered TWTT grid (Figure 4.1). Top of trap (0 value here) is at 753 m TVDss for grids AQ and AS, and at 764 m TVDss for part c). Pink points are at spill level, i.e. 26 m below top of trap for grids AS and AQ, and 17 m below top of trap for grid in part c).*

Storage volume

The migration simulations indicate that CO2 migrating in the uppermost part of the Utsira Sand (in the sand wedge) is expected to reach a major trap approximately 14 km north-northeast of the injection site. The combined storage volume in the sand wedge in the previously identified traps (Zweigel et al. 2000a) and in the large domal trap is at least 85 Million m^3, corresponding to more than 59 Million tons CO_2. This is considerably more than the planned total injection volume (20 years of injection at an annual rate of approximately 1 Million ton CO_2) and it is therefore very likely that the identified traps are large enough to store all CO_2 to be injected during the planned lifetime of the Sleipner injection project even in the case that reservoir sweep might be much less effective than presently assumed.

The assessment that enough trap volume is available for the continuation of the CO_2 injection operations is strengthened by the probable distribution of CO_2 between the two identified reservoir bodies: the main Utsira Sand and the sand wedge at the formation top. Parts of the injected CO_2 will probably be stored in traps below the 6.5 m thick shale layer (forming the base of the sand wedge) and possibly migrate towards west (Zweigel et al. 2000), whereas some other parts will migrate towards north-northeast into the domal trap identified here. The total trap volume corresponds to at least four times the planned total injection volume.

Since all CO_2 to be injected is expected to be stored in the previously and presently mapped area, it seems not to be necessary to continue detailed mapping of the reservoir top towards east.

Safety aspects

The simulations indicate that CO_2 will not migrate far from the injection site, and is not likely to reach the western or eastern margins of the basin, where sand stringers might exist in the seal unit.

Exploration well 16/7-2 is predicted to be in the area of the CO_2 accumulation if CO_2 reaches the domal trap (Figure 1.1; see Appendix A for details). Wells constitute potential pathways through the reservoir seal, and it is therefore advised that investigations be undertaken to identify its leakage potential. Possibly, measures may be taken to maintain its sealing capacity.

Provisions for monitoring

Seismic monitoring is the main, presently available method to monitor subsurface CO_2 migration and accumulation and to verify storage safety. A major prerequisite for seismic monitoring is a baseline survey, acquired prior to migration of CO_2 into the area of interest. If ongoing monitoring (especially the survey from 2003 and the one to be acquired in 2005) and related reservoir simulation should indicate that it will be likley that CO_2 will migrate out of the area of the existing 3D survey ST98M11 into the domal trap at well 16/7-2, a baseline survey covering the domal trap and the predicted migration path into it would be required.

7. References

Arts, R., Chadwick, A., Eiken, O., & Zweigel, P., 2003: Interpretation of the 1999 and 2001 time-lapse seismic data (WP5.4). TNO-report NITG 03-064-B, 32pp. (www-link)

Lindeberg, E., van der Meer, B., Moen, A., Wessel-Berg, D. & Ghaderi, A. 2000: Saline Aquifer CO_2 Storage (SACS): Final report Task 2: Fluid and core properties and reservoir simulation. Confidential report (SINTEF Petroleum Research report 54.5148.00/02/00), 43pp. Confidential. (www-link)

Sylta, Ø. 1991: Modelling of secondary migration and entrapment of a multicomponent hydrocarbon mixture using equation of state and ray-tracing modelling techniques. In: Petroleum Migration, Geol. Soc. London Spec. Publication, 59, 111-122.

Zweigel, P., Hamborg, M., Arts, R., Lothe, A., Sylta, Ø., & Tømmerås, A. 2000a: Simulation of migration of injected CO_2 in the Sleipner case by means of a secondary migration modelling tool – A contribution to the Saline Aquifer CO2 Storage project (SACS). SINTEF Petroleum Research report (CD) 23.4285.00/01/00, 63pp., 6 app., confidential. (www-link)

Zweigel, P., Lothe, A., Arts, R., & Hamborg, M, 2000b: Reservoir geology of the storage units in the Sleipner CO_2 injection case – A contribution to the Saline Aquifer CO2 Storage project (SACS). SINTEF Petroleum Research report (CD, online on SACS web) 23.4285.00/02/00, 79pp., 3 app., confidential. (www-link zip-file; www-link text only)

Zweigel, P., Bøe, R. & Lindeberg, E. 2003 (in prep): Compilation of Utsira Sand petrographic and reservoir property data acquired in the SACS project – A contribution to the Saline Aquifer CO_2 Storage (SACS) project. SINTEF Petroleum Research report 33.5324.00/04/03 – to be issued in June or July 2003.

Appendix A Migration simulation results

Appendix A.1 Case AS

a) Case AS, 2.86 Million m^3 injected

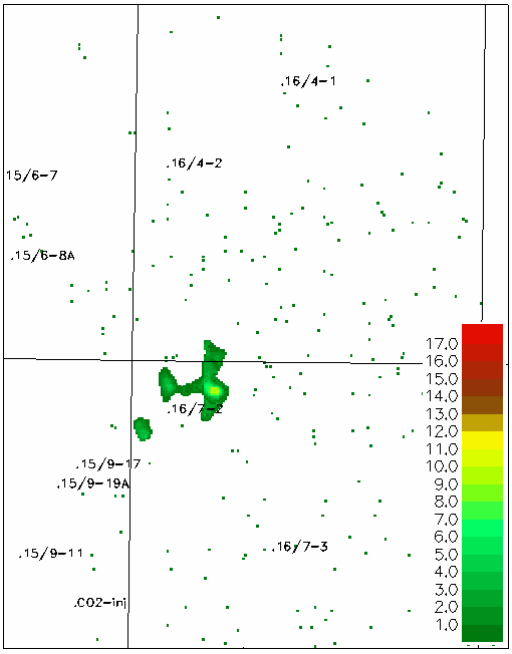

b) Case AS, 5.72 Million m^3 injected

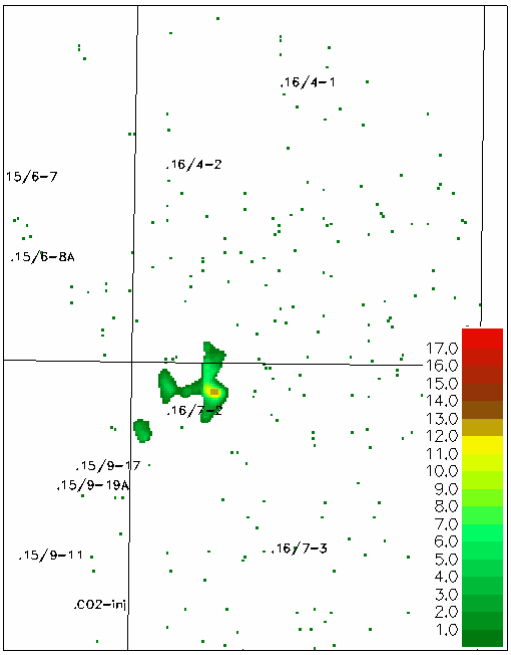

c) Case AS, 8.58 Million m^3 injected

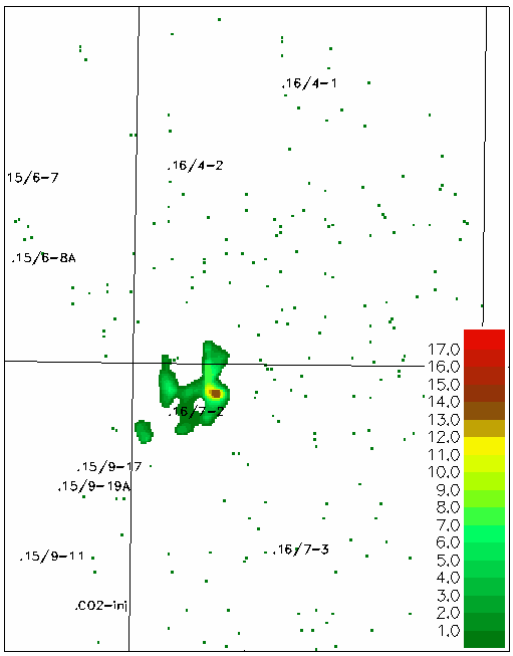

d) Case AS, 11.44 Million m^3 injected

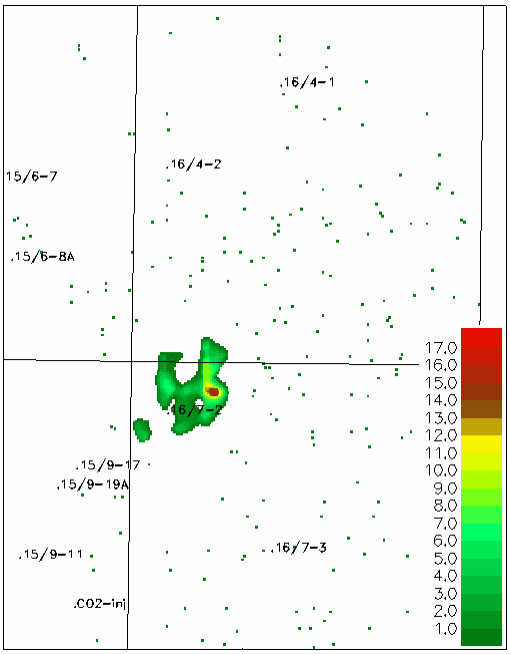

CO_2 accumulations (area and column height) simulated for case AS. Colour scale is column height in meter. For orientation use well positions and grid lines, compare to Figure 5.1. Lower figure margin is 25.9 km.

e) Case AS, 14.30 Million m^3 injected

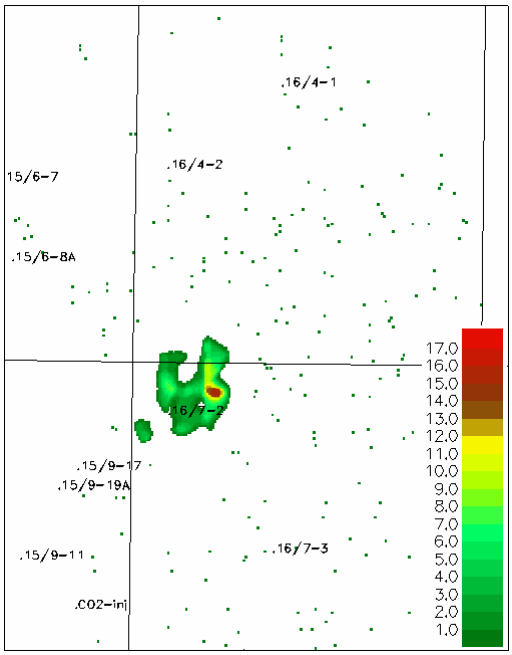

f) Case AS, 17.16 Million m^3 injected

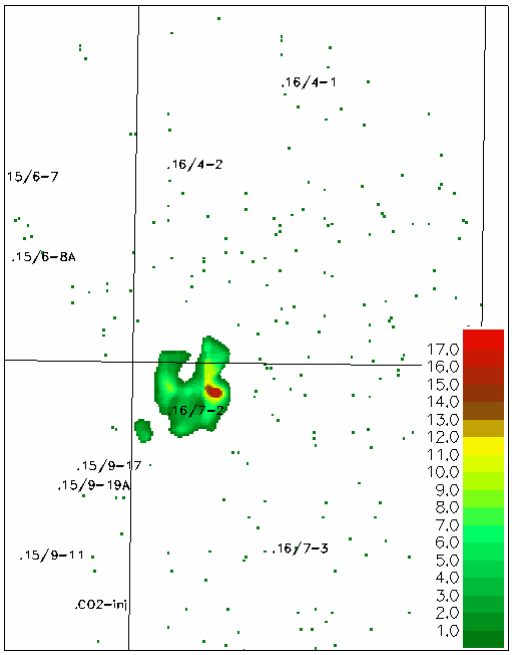

g) Case AS, 20.02 Million m^3 injected

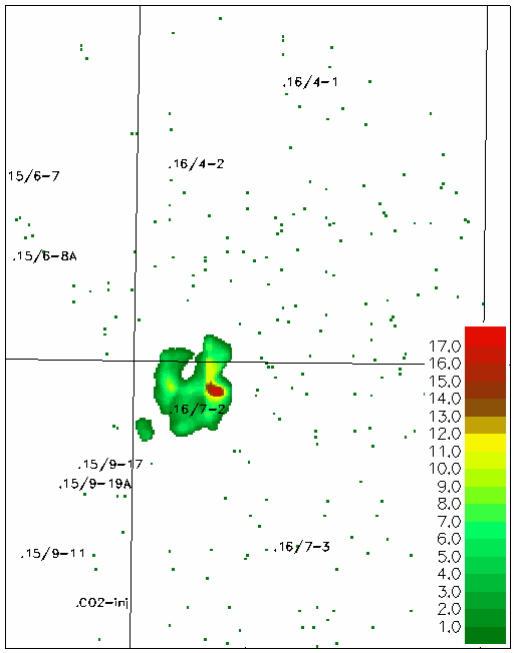

h) Case AS, 22.88 Million m^3 injected

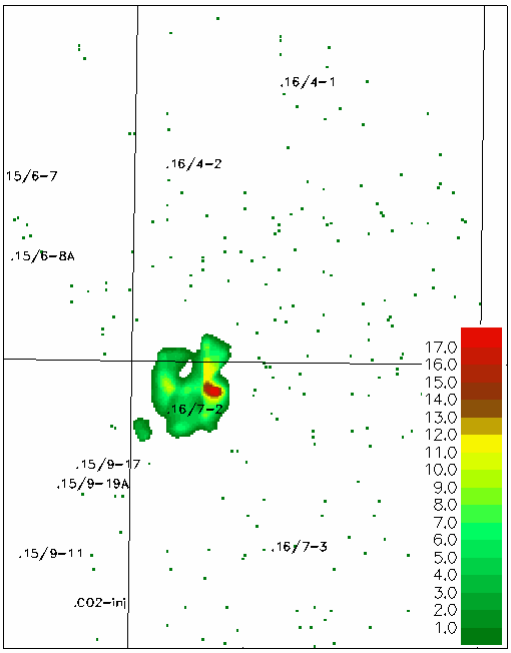

CO_2 accumulations (area and column height) simulated for case AS. Colour scale is column height in meter. For orientation use well positions and grid lines, compare to Figure 5.1. Lower figure margin is 25.9 km.

i) Case AS, 34.3 Million m^3 injected

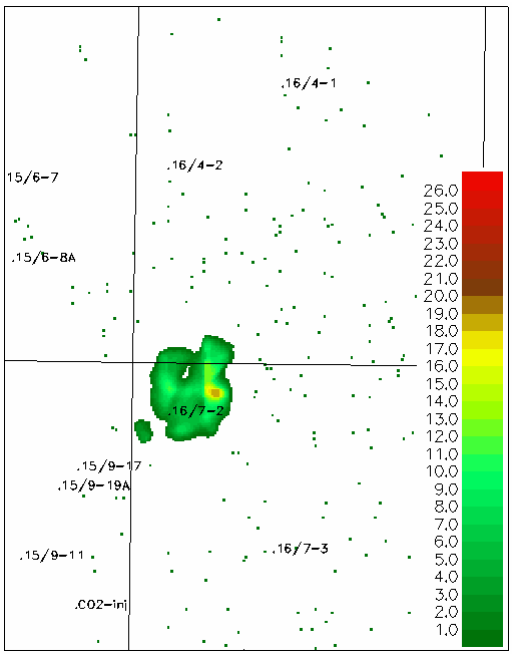

j) Case AS, 48.6 Million m^3 injected

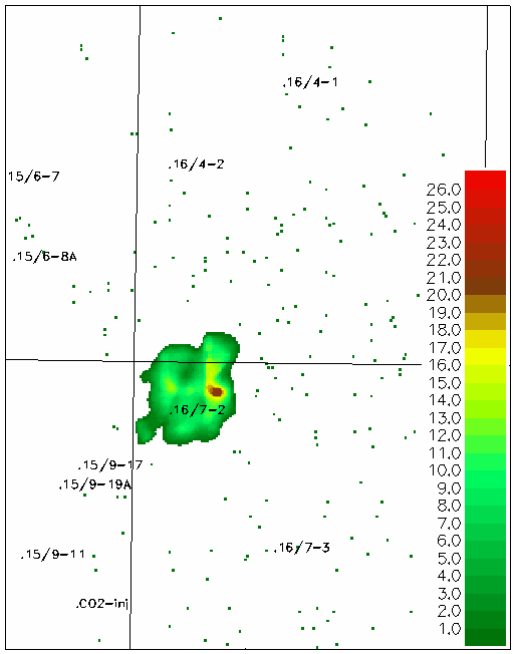

k) Case AS, 62.9 Million m^3 injected

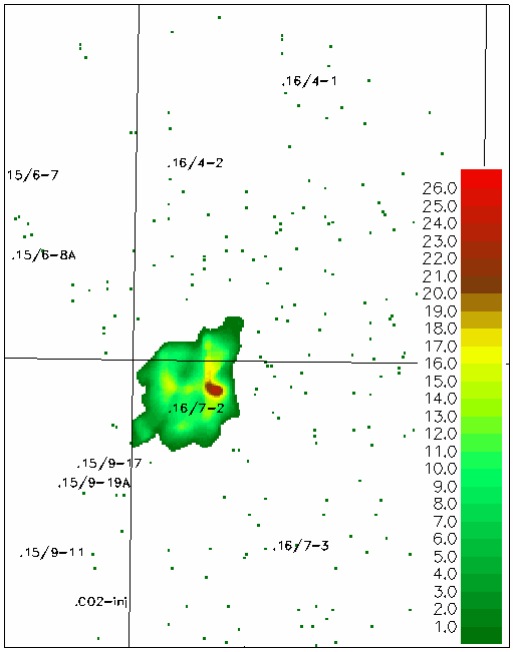

l) Case AS, 77.2 Million m^3 injected

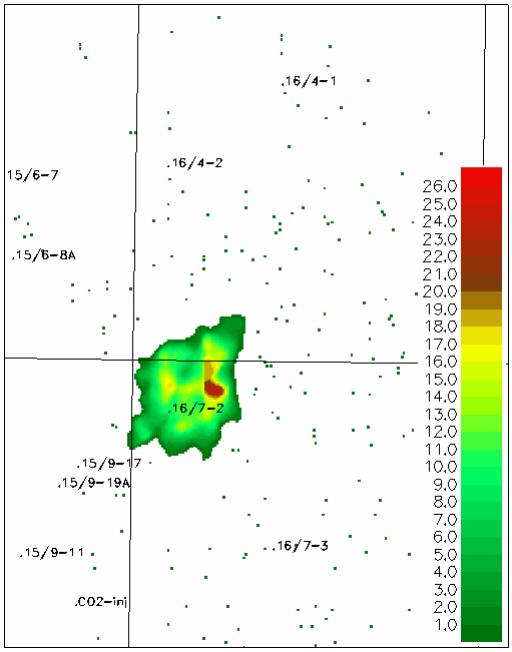

CO_2 accumulations (area and column height) simulated for case AS. Colour scale is column height in meter. For orientation use well positions and grid lines, compare to Figure 5.1. Lower figure margin is 25.9 km.

m) Case AS, 91.5 Million m^3 injected

n) Case AS, 92.0 Million m^3 injected

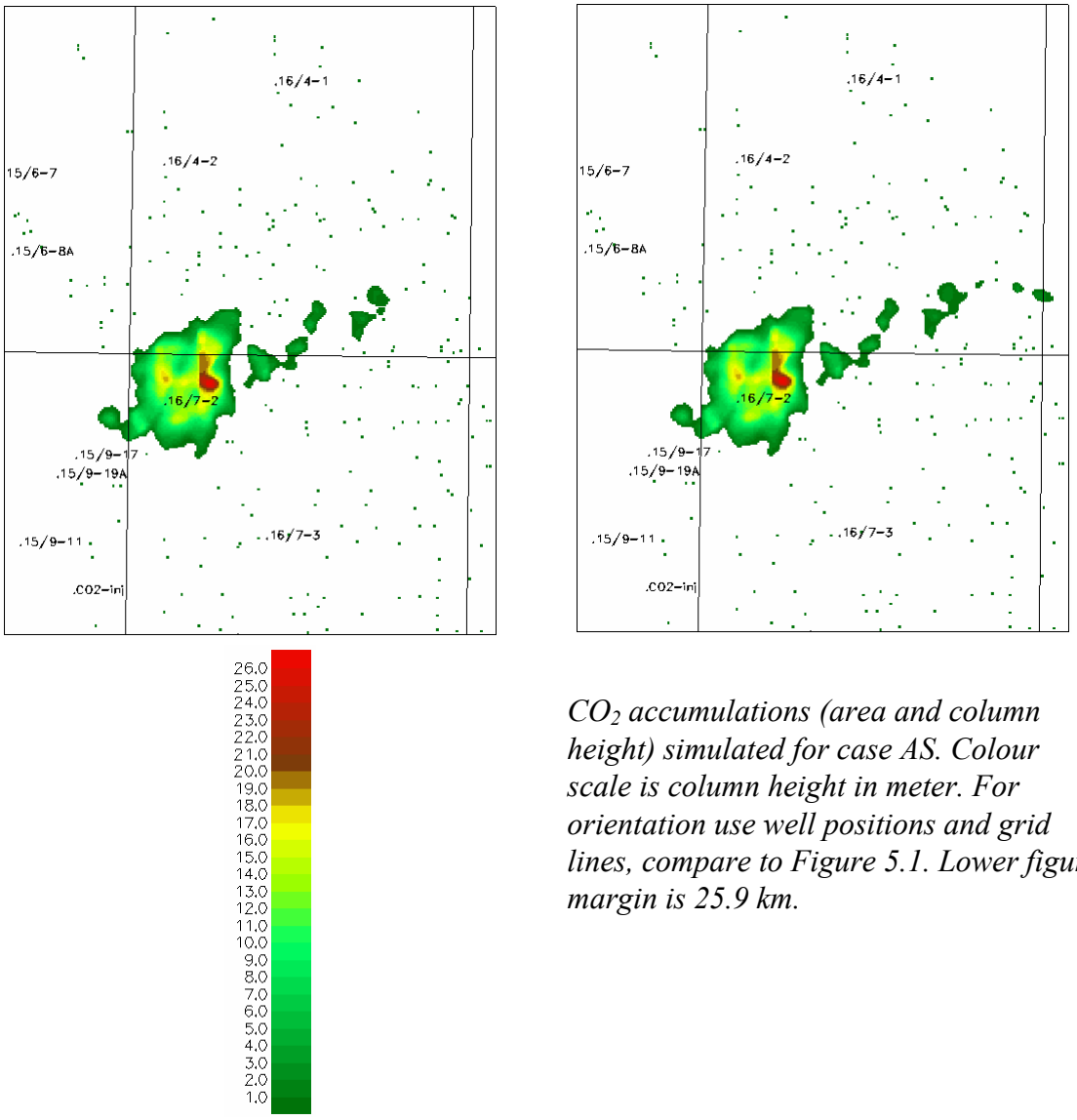

CO_2 accumulations (area and column height) simulated for case AS. Colour scale is column height in meter. For orientation use well positions and grid lines, compare to Figure 5.1. Lower figure margin is 25.9 km.

Appendix A.2 Case AQ

a) Case AQ, 2.86 Million m^3 injected

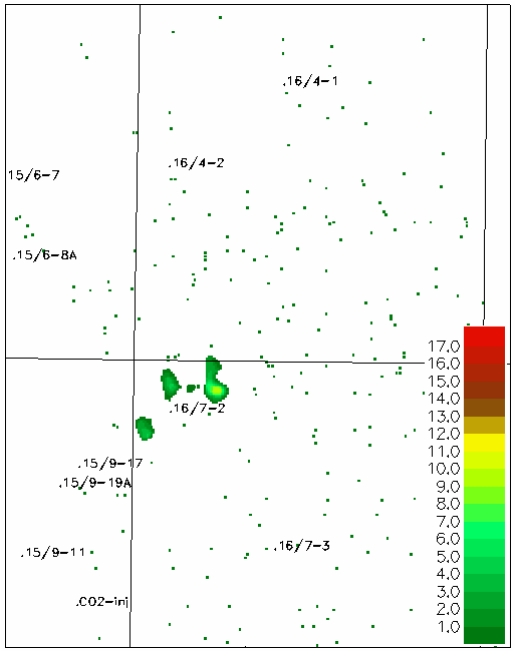

b) Case AQ, 5.72 Million m^3 injected

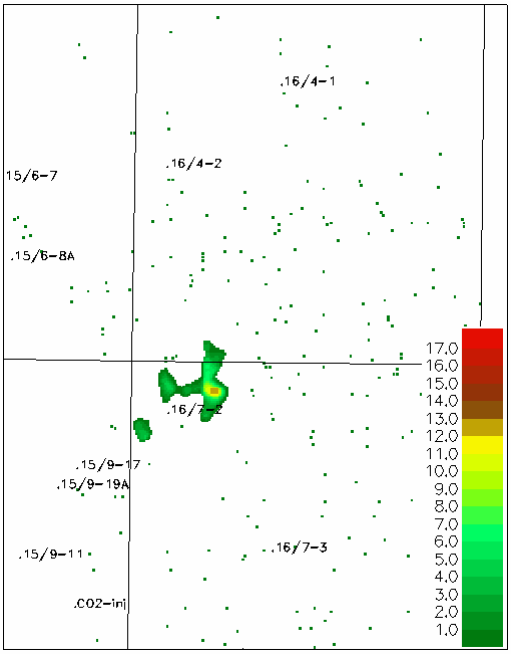

c) Case AQ, 8.58 Million m^3 injected

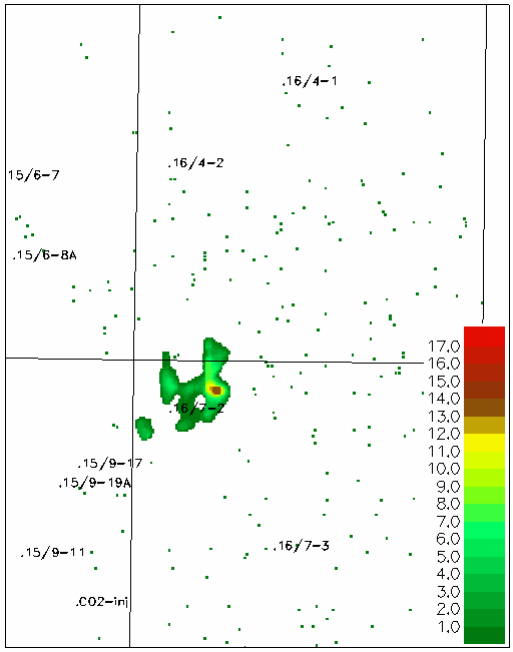

d) Case AQ, 11.44 Million m^3 injected

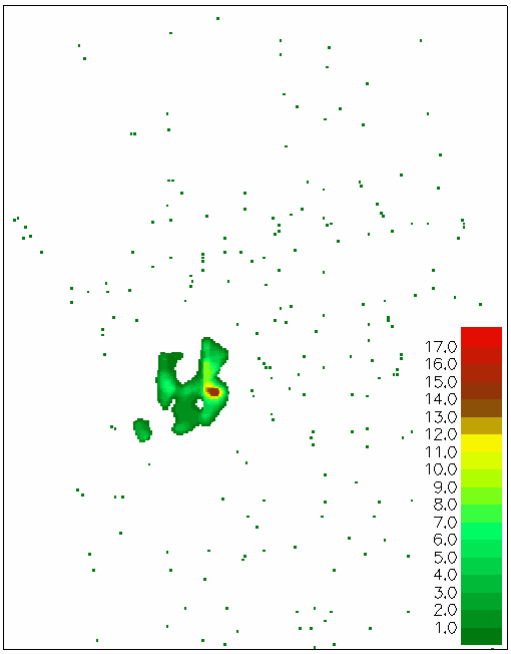

CO_2 accumulations (area and column height) simulated for case AQ. Colour scale is column height in meter. For orientation use well positions and grid lines, compare to Figure 5.1. Lower figure margin is 25.9 km.

e) Case AQ, 14.30 Million m^3 injected

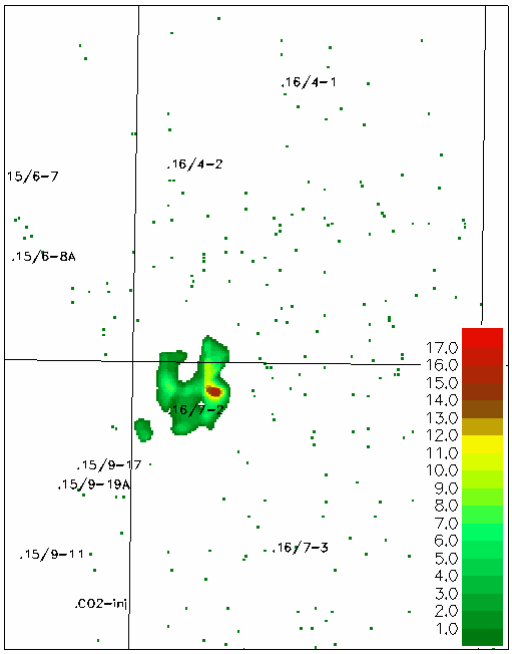

f) Case AQ, 17.16 Million m^3 injected

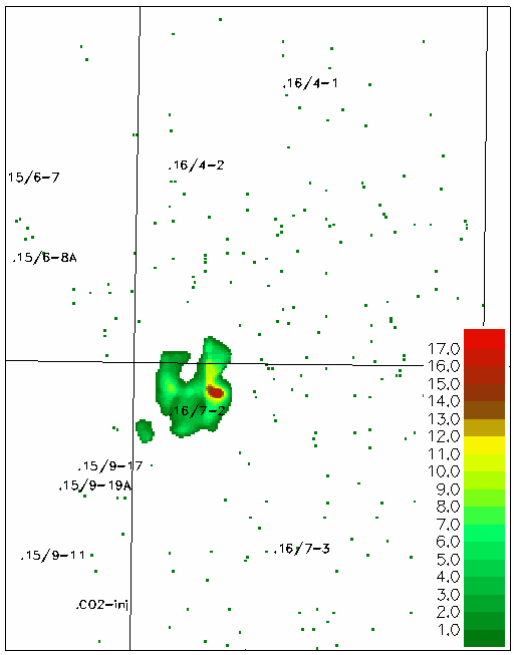

g) Case AQ, 20.02 Million m^3 injected

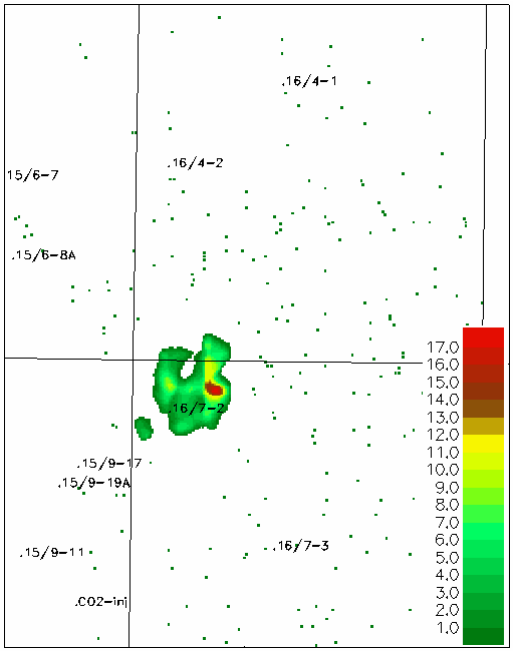

h) Case AQ, 22.88 Million m^3 injected

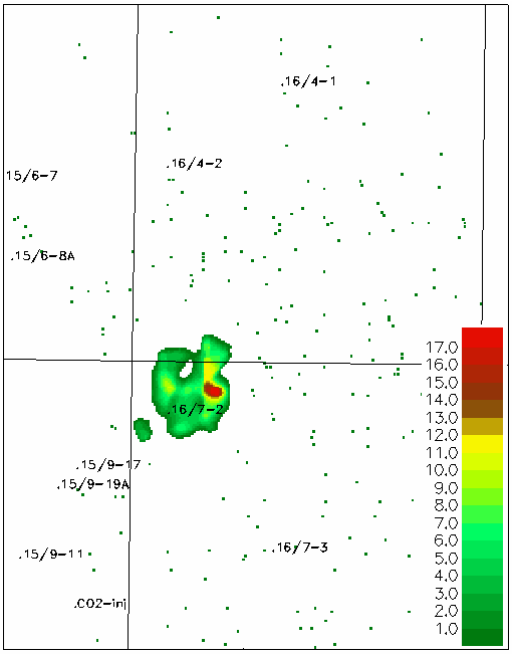

CO_2 accumulations (area and column height) simulated for case AQ. Colour scale is column height in meter. For orientation use well positions and grid lines, compare to Figure 5.1. Lower figure margin is 25.9 km.

i) Case AQ, 34.3 Million m^3 injected

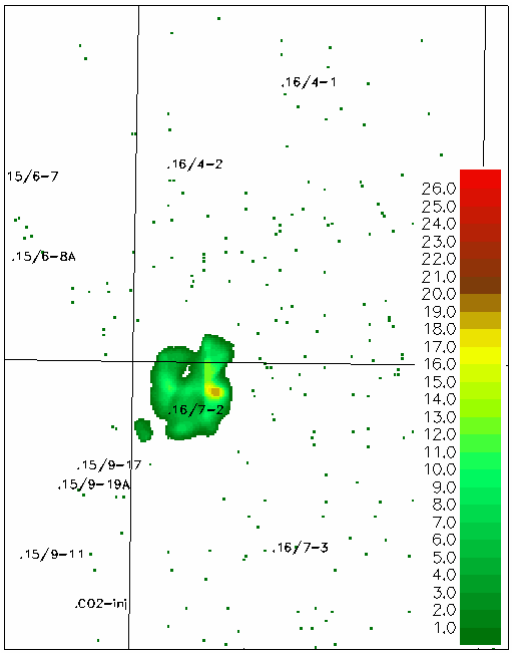

j) Case AQ, 48.6 Million m^3 injected

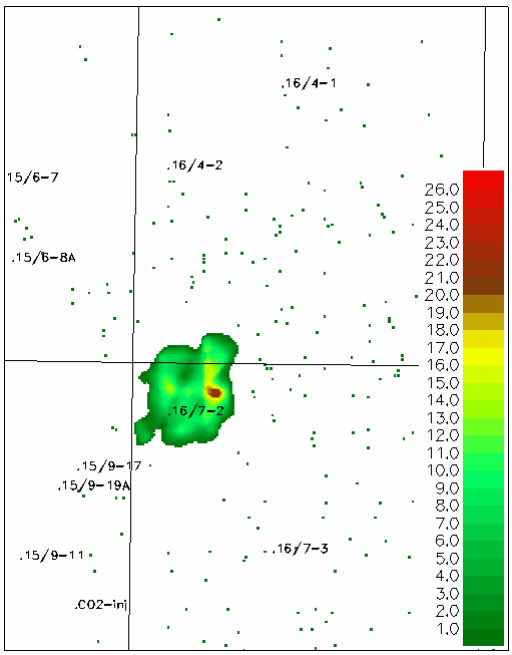

k) Case AQ, 62.9 Million m^3 injected

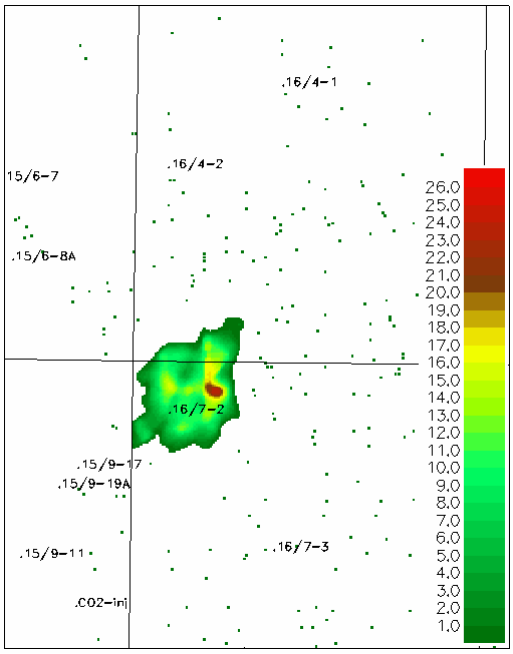

l) Case AQ, 77.2 Million m^3 injected

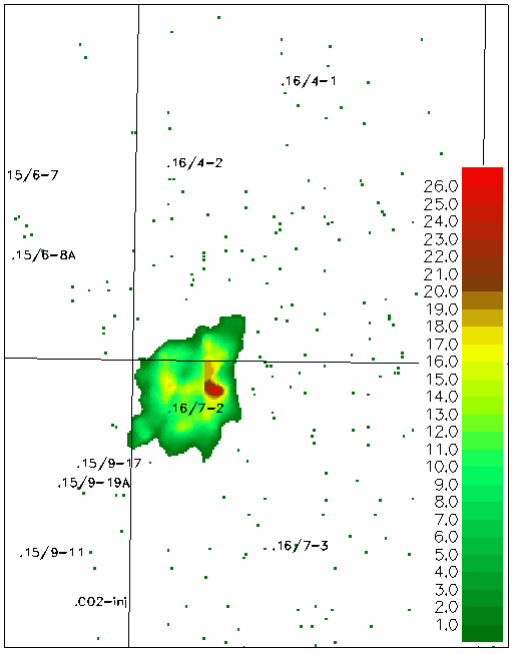

CO_2 accumulations (area and column height) simulated for case AQ. Colour scale is column height in meter. For orientation use well positions and grid lines, compare to Figure 5.1. Lower figure margin is 25.9 km.

m) Case AQ, 91.5 Million m^3 injected

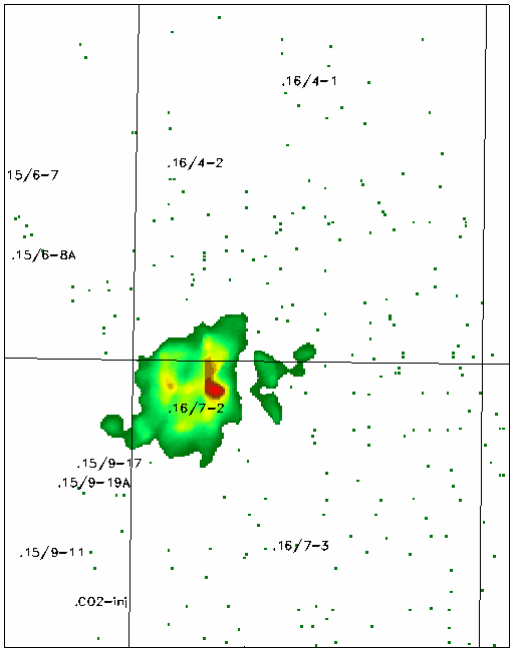

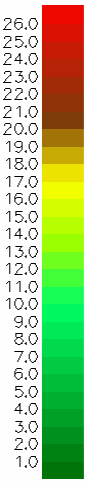

n) Case AQ, 92.0 Million m^3 injected

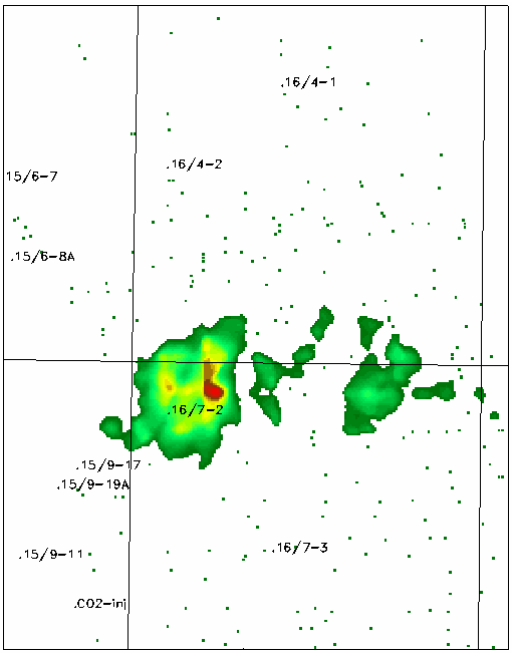

CO_2 accumulations (area and column height) simulated for case AQ. Colour scale is column height in meter. For orientation use well positions and grid lines, compare to Figure 5.1. Lower figure margin is 25.9 km.